JGR Atmospheres

RESEARCH ARTICLE
10.1029/2022JD037706

Special Section:
Advances in understanding volcanic processes

Quantification of the Volcanic Carbon Dioxide in the Air of Vulcano Porto by Stable Isotope Surveys

Roberto M. R. Di Martino[1] and **Sergio Gurrieri**[1]

[1]Istituto Nazionale di Geofisica e Vulcanologia, Sezione di Palermo, Palermo, Italy

Abstract Injecting volcanic gas into the air leads to an increase in carbon dioxide (CO_2) levels compared with background concentrations and may establish gas hazard conditions. This study reports the results of five stable isotope (i.e., $\delta^{13}C$-CO_2 and $\delta^{18}O$-CO_2) surveys of airborne CO_2 on Vulcano from August 2020 to November 2021. To measure CO_2 in the air, a mobile laboratory was equipped with a laser-based spectrophotometer that can selectively detect different CO_2 isotopologues. Volcanic CO_2 has a different isotopic signature than atmospheric CO_2 and both $\delta^{13}C$-CO_2 and $\delta^{18}O$-CO_2 can help trace the injections of volcanic gases into the air. An isotopic mass balance model was developed for partitions CO_2 between atmospheric background and volcanic CO_2. The results of these studies show that volcanic CO_2 emissions and atmospheric circulation deeply affected the concentration of CO_2 in the air at Vulcano Porto. Studies of $\delta^{13}C$-CO_2 and $\delta^{18}O$-CO_2 provide an estimate of volcanic CO_2 in the air. These results help identify spatially some points of interest for mitigating volcanic gas emission-related hazards on Vulcano.

Plain Language Summary In volcanic areas, the concentration of CO_2 in the air increases due to the dispersion of volcanic gases, as CO_2 dominates among the local gas source components. Identifying variations in gas hazard due to changes in volcanic degassing is difficult when estimates of volcanic gases in air are based only on measurements of CO_2 concentration. In this study, the effects of volcanic degassing on airborne CO_2 are thoroughly evaluated by analyzing the isotopic composition of airborne CO_2 during five onsite measurement surveys between August 2020 and November 2021. To quantify the contribution of volcanic CO_2 to total CO_2 in air, we developed a model based on the collected data using mass balance calculations. In 2021, a massive increase in volcanic degassing caused a clear increase of airborne CO_2 concentration at Vulcano. We find that the effects of volcanic degassing depend on air turbulence, which changes throughout the day. The spatial variations in CO_2 allow us to track the dispersion of volcanic gases in the air and their effects on gas hazards and atmospheric composition with unprecedented accuracy.

Key Points:

- Spatial isotope monitoring enables the identification of the origin of CO_2 in the air
- Calculating the stable isotope mass balances enables quantifying the volcanic CO_2 in the total CO_2 in the air
- Significant changes in volcanic degassing increased air CO_2 concentration and gas hazard on Vulcano—Italy—in 2021

Supporting Information:

Supporting Information may be found in the online version of this article.

Correspondence to:

R. M. R. Di Martino and S. Gurrieri,
roberto.dimartino@ingv.it;
sergio.gurrieri@ingv.it

Citation:

Di Martino, R. M. R., & Gurrieri, S. (2023). Quantification of the volcanic carbon dioxide in the air of Vulcano Porto by stable isotope surveys. *Journal of Geophysical Research: Atmospheres*, *128*, e2022JD037706. https://doi.org/10.1029/2022JD037706

Received 22 AUG 2022
Accepted 27 JUL 2023

Author Contributions:

Conceptualization: Roberto M. R. Di Martino
Data curation: Roberto M. R. Di Martino, Sergio Gurrieri
Formal analysis: Roberto M. R. Di Martino, Sergio Gurrieri
Investigation: Roberto M. R. Di Martino, Sergio Gurrieri
Methodology: Roberto M. R. Di Martino
Resources: Roberto M. R. Di Martino, Sergio Gurrieri

1. Introduction

Atmospheric CO_2 plays a critical role in the greenhouse effect and, along with water vapor, helps maintain an appropriate atmospheric temperature that makes Earth a habitable planet. Both the atmosphere and the oceans are CO_2 sinks (Behrenfeld et al., 2006; Berner, 2003; Bottinga & Craig, 1969; Ciais & Meijer, 1998; Sabine et al., 2004). In the long term, increases in seawater temperature promote the release of CO_2 from the oceans and thus enhance the greenhouse effect (Harries et al., 2001; Lacis et al., 2010; Li & Elderfield, 2013). In the short term, the increase in CO_2 emissions depends on various human activities (Andrew, 2018; Calvert et al., 1993; Hasambeigi et al., 2012; Paraschiv & Paraschiv, 2020; Wimbadi et al., 2021) that increase the concentration of CO_2 in the air. The recent trend in carbon dioxide emissions has been the subject of many studies, as global warming leads to more frequent heavy rainfall events, thunderstorms, an increase in air temperature, frequent flooding in tropical regions, severe drought events in desert regions, sea level rise, and landslides. These events are an expression of the current climate warming (Giorgi et al., 2011, 2018; Hennessy et al., 1997; Rogger et al., 2022; Scoccimarro et al., 2013; Torres et al., 2022; Umair et al., 2020; Wu et al., 2020; Xu et al., 2019).

Despite the importance of CO_2 in the atmosphere, there are still few direct measurements of CO_2 flux, whether from anthropogenic or natural sources. Attempts to partition CO_2 emissions are based on a combination of carbon content in hydrocarbons and fossil fuel consumption statistics (Wimbadi et al., 2021; Yaacob et al., 2020). Although several studies have recognized that volcanic CO_2 affects air quality, there is relatively little isotope-based literature that examine the source of airborne CO_2 emissions at high spatial resolution in urban areas (Capasso et al., 2019, 2021; Di Martino & Capasso, 2019, 2021 and reference therein). Volcanoes emit large amounts of

Software: Roberto M. R. Di Martino
Supervision: Roberto M. R. Di Martino, Sergio Gurrieri
Validation: Roberto M. R. Di Martino, Sergio Gurrieri
Visualization: Roberto M. R. Di Martino, Sergio Gurrieri
Writing – original draft: Roberto M. R. Di Martino
Writing – review & editing: Roberto M. R. Di Martino, Sergio Gurrieri

CO_2 through crater plumes (Aiuppa et al., 2019; Burton et al., 2013), fumaroles (Capasso et al., 1997; Chiodini et al., 1991; Di Martino, Camarda, et al., 2016; Di Martino et al., 2013, 2021a, 2021b; Federico et al., 2023; Italiano & Nuccio, 1992; Paonita et al., 2002), and groundwater (Capasso et al., 2017). Diffuse degassing occurs throughout the volcanic edifice (Badalamenti et al., 1988; Carapezza et al., 2011; Di Martino et al., 2020), and variations in soil CO_2 flux (φCO_2) have helped track either fluctuations in volcanic activity at open conduit volcanoes or the transition to a period of unrest at dormant volcanoes (Camarda et al., 2019; Di Martino, Camarda, et al., 2016; Di Martino et al., 2013; Gurrieri et al., 2008, 2021; Melián et al., 2014). Although φCO_2 correlates with volcanic activity, φCO_2 also occurs in zones of active faulting, suggesting that the Earth's crust has some degree of permeability to gases. Therefore, lateral variations in φCO_2 have helped to identify hidden faults (Camarda et al., 2020) and investigate stress variations in the crust (Camarda et al., 2016).

For several decades, φCO_2 has been routinely studied in volcanic areas (Badalamenti et al., 1991; Camarda et al., 2006a, 2006b; Carapezza & Federico, 2000; Chiodini et al., 1996, 1998; Diliberto et al., 2002), and several attempts have been made to partition φCO_2 between volcanic and biological origin (Di Martino, Capasso, & Camarda, 2016; Di Martino et al., 2020; Viveiros et al., 2020). The estimation of φCO_2 is important for both volcano monitoring and risk management due to either volcanic unrest or toxic gas emission in poorly ventilated areas. Although the stable isotope signature of the local CO_2 source can help understand how volcanic emissions affect airborne CO_2 concentrations (Viveiros et al., 2008), there are few constraints from isotopic monitoring in volcanic areas (Di Martino & Capasso, 2019, 2021; Di Martino and Gurrieri, 2022b, 2022a, 2023; Venturi et al., 2019).

Since 1988, researchers have estimated volcanic CO_2 in the air on Vulcano either by measuring CO_2 concentration or by measuring SO_2 flux scaled by the CO_2/SO_2 mass ratio (Tamburello et al., 2011; Vita et al., 2012). The limitation of these approaches arises from the fact that CO_2 is the fourth most abundant constituent in the atmosphere, making it difficult to detect concentration anomalies relative to the local atmospheric CO_2 background. In this paper, we discuss the spatial variations of volcanic CO_2 in the air using measurements of CO_2 concentration integrated by stable isotopes in air CO_2 (i.e., $\delta^{13}C$-CO_2 and $\delta^{18}O$-CO_2). The main advantage of using stable isotopes in CO_2 in addition to CO_2 concentration measurements is that volcanic CO_2 can be effectively distinguished from CO_2 in air, because both $\delta^{13}C$-CO_2 and $\delta^{18}O$-CO_2 of volcanic CO_2 are different from those of the atmospheric CO_2 background (Yakir, 2003). This study aims to quantify the effects of changes in volcanic gas emissions on atmospheric CO_2 at Vulcano, Aeolian Island - Italy. Since late September 2021, volcanic degassing on Vulcano has suddenly increased, prompting civil protection authorities to change the alert level from "green" to "yellow." The mitigation of the gas hazard includes several measures in the populated zones of Vulcano Porto. Integrated monitoring of φCO_2 and airborne CO_2 concentrations plays a central role in gas hazard assessment (Camarda et al., 2023; Di Martino et al., 2021b; Gurrieri et al., 2022). However, spatial and temporal monitoring of isotopes in airborne CO_2 allows quantifying the impact of volcanic degassing on air quality and gaining a deeper understanding of gas-hazard zones during a period of increasing volcanic degassing. The integrated analysis of stable isotopes in CO_2 (i.e., carbon and oxygen) allowed the estimation of the volcanic contribution to atmospheric CO_2.

2. Study Area

Vulcano, Stromboli, Lipari and Panarea are active volcanoes on the Aeolian Islands in the Tyrrhenian Sea near the northern coast of Sicily—Italy (Figure 1), characterized by different types of volcanic activity. Stromboli erupts shoshonitic magma through almost continuous strombolian explosions, while Panarea shows sudden gas releases interrupting the quiet submerged degassing. Vulcano exhibits medium energy explosions (i.e., VEI ranges from 2 to 3) that interrupt quiescent degassing. The NW–SE oriented Tindari-Letojanni fault system (Figure 1b) vertically conducts both fluids and magma onto Vulcano (Barreca et al., 2014; Chiarabba et al., 2008; De Astis et al., 2003, 2013; Forni et al., 2013; Palano et al., 2012). The extinct eruptive centers on Vulcano show an orientation consistent with this fault direction. The La Fossa cone was formed after the most recent eruptions in the Fossa caldera and is located at the intersection of the Tindari-Letojanni and the conjugate NE–SE fault systems. The last eruption at La Fossa crater of Vulcano occurred between 1888 and 1890 and marked the transition to the present solfataric activity.

Fumaroles at La Fossa crater, Levante beach, and Faraglione, as well as thermal groundwater, are some of the manifestations of volcanic fluids that rise on Vulcano (Chiodini et al., 1998; Nuccio et al., 1999). Mud pools and sulfur deposits occur near Faraglione. The φCO_2 in the La Fossa caldera zone sometimes has a carbon isotope signature similar to the fumarolic CO_2 in the crater (Capasso et al., 1997; Paonita et al., 2002). Anomalous zones

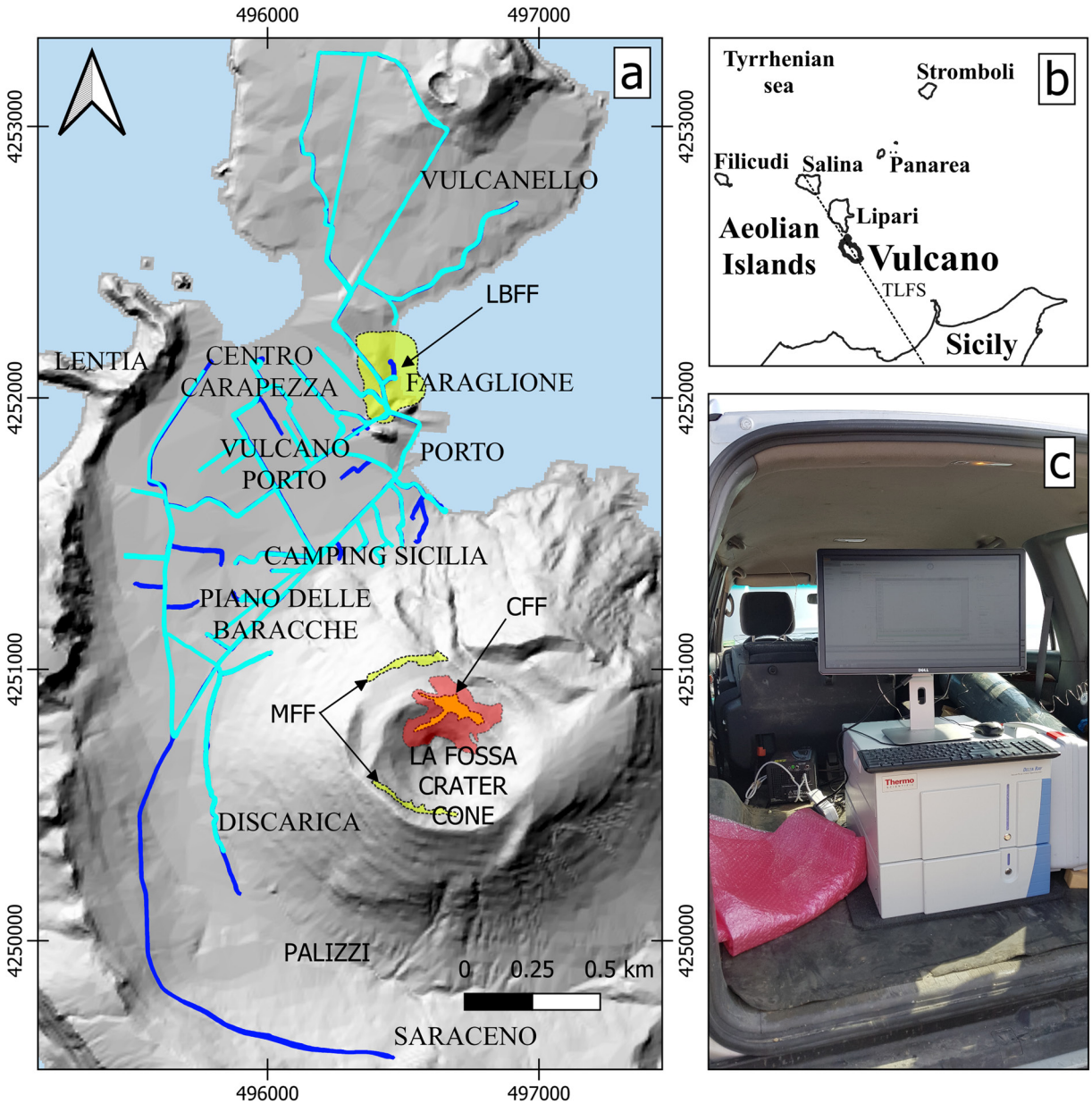

Figure 1. (a) Route through the village of Vulcano Porto on the island of Vulcano; the light blue line shows the planned route for the August 2020 to November 2021 surveys. In addition to the usual route followed during previous surveys, the additional routes marked with blue color were followed in November 2021. Basemap DEM from Tinitaly (Tarquini et al., 2023). The main crater fumarolic field (CFF), the minor fumarolic area (MFF) in the crater cone and the fumarolic field at Levante beach (LBFF) are shown; (b) the island of Vulcano and the Aeolian Archipelago in the Tyrrhenian Sea, north of the island of Sicily, Italy. TLFS shows the Tindari-Letojanni fault system; (c) the mobile laboratory equipped with Thermo Fisher Scientific's Delta RayTM and instruments during the survey on Vulcano.

of φCO_2 have a stable position at Faraglione and Palizzi (Camarda et al., 2006a, 2006b), although remarkable variations in φCO_2 magnitude have been systematically correlated with changes in volcanic degassing. More specifically, significant increases in φCO_2 (i.e., 10%–50% compared to CO_2 emissions from the crater) occurred at these anomalous degassing zones, coinciding with "crises" that interrupted the solfataric degassing of La Fossa volcano (Chiodini et al., 1996, 1998; Granieri et al., 2006; Nuccio et al., 1999; Paonita et al., 2013).

The stable isotopic composition of CO_2 in air helps track variations in the local sources of gas emissions (Di Martino and Gurrieri, 2022a, 2022b).

Volcanic gas dispersion depends on air turbulence, which is influenced by insulation, albedo, wind speed, and wind direction. Primarily, wind speed indicates the degree of air turbulence, while wind direction affects CO_2

concentration in different zones of the island. Several aspects of the island of Vulcano can affect air circulation and have dramatic effects on air quality. First, the island of Vulcano hosts the active volcano La Fossa, which is a strong source of volcanic CO_2 and other chemical compounds (e.g., sulfur dioxide, SO_2, and hydrogen sulfide, H_2S) that can be toxic to island residents. In addition, the differential heating of land and sea water results in a cyclic wind pattern that drives air from sea to land during the day. At night, the wind is said to reverse and blow from the land to the island and back to the sea. However, this schematic pattern in the inhabited zone of Vulcano Porto is further complicated by the morphology of the caldera. In fact, the inhabited zone of Vulcano Porto develops between the flank of the volcanic cone to the south-east and Mount Lentia to the west, at the foot of a canyon-like topographic structure that does not facilitate air circulation. CO_2 has a density higher than air, so it can accumulate in the lower layers of the atmosphere and reach high concentrations near the ground. In addition, CO_2 is an odorless gas and therefore poses a greater hazard than H_2S, another volcanic gas component released on Vulcano (Carapezza et al., 2011). Although CO_2 rarely reaches concentrations greater than 1,000 ppm vol in the air due to non-volcanic processes, only the stable isotopic signature of CO_2 can provide information about its origin in the air (i.e., biogenic, anthropogenic, and volcanic CO_2).

3. Materials and Methods

3.1. Instrument Setup

The instrument used to acquire data discussed in this paper is a Delta Ray—Thermo Fisher Scientific. It measures the concentration of the isotopologues ^{13}COO, ^{12}COO, and $CO^{18}O$ based on the strength of adsorption of light in the mid-infrared region (~4.3 μm) according to the Lambert-Beer law. Both the $^{13}C/^{12}C$ and $^{18}O/^{16}O$ ratios are calculated by different concentration ratios of the isotopologues, while the total CO_2 concentration is obtained by summing the concentration of the three CO_2 isotopologues. The stable isotope ratios refer to the Vienna Pee Dee Belemnite (VPDB) international standard and are expressed by the δ-notation (i.e., $\delta^{13}C\text{-}CO_2$ and $\delta^{18}O\text{-}CO_2$, respectively) in the CO_2 concentration range of 200–3,500 ppm vol.

The Delta Ray instrument is supplied with the QTegra software. A specially designed template includes protocols for recording $\delta^{13}C\text{-}CO_2$, $\delta^{18}O\text{-}CO_2$, and CO_2 concentration values, as well as information on the list of samples, acquisition parameters, referencing, evaluation settings, and sample definition. Instrument calibration and referencing of measurements against two working standards provides ±0.25 ‰ accuracy for isotope determinations and ±1 ppm vol accuracy for CO_2 concentration measurements. The QTegra software performs instrument calibration based on one of two working standards (Table S1 in Supporting Information S1) and establishes a correlation between adsorption strength and concentration by diluting with CO_2-free synthetic air. A second calibration procedure allows correlation of the raw $\delta^{13}C\text{-}CO_2$ and $\delta^{18}O\text{-}CO_2$ values with the expected range of isotopic composition of the unknown gas sample by using a second working standard (Table S1 in Supporting Information S1).

The instrument records each measurement of $\delta^{13}C\text{-}CO_2$ and $\delta^{18}O\text{-}CO_2$ at a frequency of 1 Hz. Prior to data acquisition, the instrument performs isotope ratio referencing on the working standards at a fixed CO_2 concentration (i.e., CO_2 = 400 ppm vol.; 720 mg m^{-3}) that approximates background CO_2 in the air. After the unknown air sample is purged for 60 s, the instrument skips the purge and measures the concentration of CO_2 isotopologues in the air. Once the air has purged the gas inlet, the instrument calculates $\delta^{13}C\text{-}CO_2$ and $\delta^{18}O\_CO_2$ as well as CO_2 concentration.

3.2. Measurement Strategies

An off–road vehicle housed the instrument, the gas tank (i.e., both the $\delta^{13}C\text{-}CO_2$ and $\delta^{18}O\text{-}CO_2$ working standards and the CO_2-free synthetic air), and the equipment to measure $\delta^{13}C\text{-}CO_2$, $\delta^{18}O\text{-}CO_2$, and airborne CO_2 concentrations during the studies on Vulcano. The positioning of the vehicle was recorded by a global positioning system device (GARMIN GPSMAP® 64s) time synchronized with the Delta Ray's internal clock.

An inverter (12 V input-output, pure sine wave) was connected to the car's electrical system, which supplied power to the instrument (~300 W). A stainless-steel capillary (1/16 in.; Swagelok-type™, 3 m long) was connected to the inlet of the instrument, while the other side of the tube was attached to the front of the car roof (~2.3 m above the ground) to avoid possible contamination from the gasoline engine exhaust. The air was passed through a filter (2 μm, 1/16 in, capillary aperture) to avoid contamination from dust moving through the roads.

Table 1
Statistics of the Data set Collected in the Field (Di Martino and Gurrieri, 2022a, 2022b)

Survey	Number of measurements	Start time (hh:mm:ss)	End time (hh:mm:ss)	$\delta^{13}C\text{-}CO_2$ (‰ vs. VPDB)			$\delta^{18}O\text{-}CO_2$ (‰ vs. VPDB)			CO_2 concentration (ppm vol)			Wind speed during survey (m s^{-1})
				Min	Average	Max	Min	Average	Max	Min	Average	Max	Average
5 August 2020	1,417	08:37:01	09:01:44	−12.99	−8.13	−3.42	−8.15	−2.69	0.49	410	418	555	0.15
16 June 2021 (AM)	589	10:44:29	12:22:19	−11.55	−9.09	−7.31	−5.59	−2.81	−1.30	402	409	459	0.36
16 June 2021 (PM)	546	17:53:58	19:24:44	−11.42	−9.05	−7.6	−4.74	−2.10	−0.50	405	411	490	0.23
19 October 2021	7,801	09:59:28	12:24:53	−12.55	−7.89	−3.16	−5.76	−1.30	2.60	418	435	569	0.19
23 November 2021	10,852	09:19:46	12:31:05	−14.17	−8.83	−3.02	−8.60	−2.18	3.60	419	446	1,121	0.28

Note. Wind speed data are from Vita Fabio (personal communication).

A route of about 20 km was designed in the laboratory, using the island's roads and some accessible off-road path, covering different environments of the caldera such as coastal areas, cone flanks and residential areas (i.e., Vulcano Porto, including the base of Lentia, Discarica, Palizzi, Rimessa, Faraglione, Istmo, and Vulcanello). The course of the route was planned in such a way that the segments of the route do not overlap, so as not to increase the statistical weight of some route segments over others. The route was closely followed using a routing application (e.g., Google Maps). Each survey was completed in 2 hours of continuous measurements, and the spatial density of measurements corresponded to the metric order scale (~3 m average distance between measurements). The data set includes ~21200 georeferenced measurements for $\delta^{13}C\text{-}CO_2$, $\delta^{18}O\text{-}CO_2$, and CO_2 concentration, respectively (Di Martino and Gurrieri, 2022a, 2022b). Since August 2020, five surveys have been conducted at Vulcano to test and refine the measurement method. In August 2020 and June 2021, the measurements allowed us to study the dispersion of volcanic CO_2. The results of this investigation will allow comparison with the data set collected in October and November 2021, when degassing had already increased.

3.3. Data Processing Approach

The data obtained through the onsite measurements were processed using the Keeling plot approach and mass balance models for oxygen and carbon isotopes.

The Keeling plot allows identification of the dominant source of CO_2 at the local scale using observational data. The mass balance model for oxygen and carbon isotopes aims to quantify the impact of the CO_2 source on the air at the local scale. The algebraic equations of the model were developed as part of this study and are described in the section of this paper dealing with the assessment of volcanic CO_2 in the air at Vulcano Porto (see Section 5.2). This approach combines measurements of the stable isotopes of CO_2 in the air with isotopic signatures of both the local CO_2 source (Table S2 in Supporting Information S1), as determined by the Keeling plot method (Keeling, 1958), and CO_2 in the background air. The theoretical results of the model allow the CO_2 in the air to be partitioned between the local background air and the CO_2 source. In the specific case of Vulcano Island, we focused on the assessment of volcanic CO_2, since this is the main source of CO_2 in the air of Vulcano Porto. The measurements used in the theoretical results of the model (i.e., see Equation 10 of this study) provide the volcanic CO_2 concentration (C_V) point by point of the path. After this calculation, the interpolation of the C_V values using the Kriging algorithm with spherical autocorrelation model provided simulations of volcanic CO_2 dispersion. This algorithm provided the prediction layer for $\delta^{13}C\text{-}CO_2$, $\delta^{18}O\text{-}CO_2$, CO_2 concentration, and C_V based on the assumption that each interpolating variable changes linearly with the distance between adjacent measurements. The spherical model has the advantage that the interpolation asymptotically reaches the autocorrelation distance (i.e., the distance at which two adjacent measurements are statistically uncorrelated). Using the spherical model in this study, we based on the assumption that spatial distribution of measurements is fairly homogeneous on a metric scale, which is consistent with the expected magnitude of spatial variations in atmospheric variables at the local scale (Oke et al., 2017). Simulations of stable isotope variables, airborne CO_2 concentration, and volcanic CO_2 dispersion were performed using the Quantum GIS software package.

4. Results

In 2021, Vulcano experienced a significant increase in volcanic outgassing (Aiuppa et al., 2022; Di Martino et al., 2022; Federico et al., 2023; Inguaggiato et al., 2022). Although Vulcano has not yet produced a volcanic eruption, the Italian civil protection authorities (DPC) prohibited access to some zones of the island where high φCO_2 caused a sharp increase in the gas hazard. Soil gas measurements showed that φCO_2 levels increased almost 10 times their original value from September to November 2021 at Vulcano Porto (Di Martino et al., 2022).

This study shows the results of five surveys conducted on the island of Vulcano to measure the spatial variations of CO_2 in the air before and during the volcanic crisis in 2020 and 2021, respectively. Table 1 provides a statistical summary of the data discussed in this study and an overview of the wind speed during each survey (i.e., average wind speed by Vita F., personal communication), while the CO_2 database is available online (Di Martino & Gurrieri, 2022a). These surveys were conducted under wind speed in the range of light air (i.e., from 0.15 to 0.36 m s^{-1}), while the average value of the wind speed during our survey was 0.24 m s^{-1}.

4.1. $\delta^{13}C$ of the Air CO_2 and CO_2 Concentration

Measurements of $\delta^{13}C\text{-}CO_2$ and $\delta^{18}O\text{-}CO_2$ are used to assess the hazards associated with variations in airborne CO_2 concentrations and the societal consequences of increasing volcanic degassing. The $\delta^{13}C\text{-}CO_2$ value exhibited significant spatial variations during each survey on Vulcano, and the average value of airborne CO_2 concentration was significantly higher during the 2021 crisis compared to those of the pre-crisis period. Figure 2a shows the statistics of CO_2 concentration in air on 5 August 2020 (dashed bars) in comparison with $\delta^{13}C\text{-}CO_2$ (filled bar). Measurements were carried out during the day (i.e., between 8:37 and 10:00 a.m. local time) and the most abundant $\delta^{13}C\text{-}CO_2$ values indicate that carbon of CO_2 was slightly less ^{13}C-depleted (i.e., −8.5‰ vs. VPDB) than standard air. In this paper, the value of 741 mg m^{-3} (i.e., CO_2 concentration = 412 ppm vol) was chosen for the CO_2 concentration of standard air with $\delta^{13}C\text{-}CO_2 = -8.0$‰ versus VPDB and $\delta^{18}O\text{-}CO_2 = -0.1$‰ versus VPDB as its nominal isotopic signature. The selection of these values in the CO_2 distribution model (i.e., see Section 5.2 of this study) leads to a conservative estimate of volcanic CO_2 in the air of Vulcano Porto. The distribution of the data set shows that ∼75% of the CO_2 concentration values were lower than 420 ppm vol (720 mg m^{-3}), while a few percent (i.e., <2%) were higher than 450 ppm vol (810 mg m^{-3}), up to 456 ppm vol. The comparison with the value of standard air shows that the local CO_2 source influences the CO_2 concentration in the air on Vulcano. The nearly symmetric distribution of $\delta^{13}C\text{-}CO_2$ indicates that both less ^{13}C-depleted (i.e., volcanic CO_2) and more ^{13}C-depleted (i.e., human-caused CO_2 emissions) contribute to CO_2 in the air on Vulcano. Human-caused CO_2 emissions are not expected to significantly pollute the air on Vulcano. However, the growing population on the island and traffic with internal combustion engines may pollute the air on Vulcano during the summer months. A power plant that supplies ∼180 KW to the island of Vulcano is located at Piano delle Baracche and emits CO_2 into the atmosphere from the combustion of hydrocarbons. The $\delta^{13}C\text{-}CO_2$ data set shows that a ^{13}C-enriched CO_2 source influenced the spatial variations of CO_2 in the air (Di Martino & Gurrieri, 2022a). In August 2020, CO_2 concentrations slightly higher than standard air were almost ubiquitous at Vulcano Porto. The highest concentrations were found in a broad zone near Lentia, in some areas in the central part of Vulcano Porto, and in Vulcanello. CO_2 concentrations exceeded 420 ppm vol. at Porto and Faraglione. The data set collected on 16 June 2021 during two surveys allows a comparison between the morning hours (i.e., from 10:44 to 12:22 local time) and the late afternoon (i.e., from 17:53 to 19:24 local time) for the $\delta^{13}C\text{-}CO_2$. The two-peaked distribution of $\delta^{13}C\text{-}CO_2$ values during the morning hours (Figure 2b) has the less ^{13}C-depleted peak consistent with the carbon isotope composition of standard air (i.e., $\delta^{13}C\text{-}CO_2 = -8$‰ vs. VPDB).

The second peak has a more negative $\delta^{13}C\text{-}CO_2$ value, indicating a local CO_2 source with a more negative $\delta^{13}C\text{-}CO_2$ signature. Data collected in the afternoon show a unique peak with a $\delta^{13}C\text{-}CO_2$ signature lower than that of standard air, with a long tail end to $\delta^{13}C\text{-}CO_2 \approx -14$‰ vs. VPDB. Figure 3b shows a punctuated spatial variation of CO_2 concentration in the air at Vulcano Porto, where several zones of high concentration are seen during the morning hours, while two rather homogeneous zones of high concentration persisted during the afternoon period (Figure 3c). The spatial variations in air CO_2 concentration reveal differences in the stability of the lower atmospheric layer in the morning and afternoon. Solar radiation promotes air turbulence in the morning hours due to atmospheric warming. The air turbulence disturbs the stratification of the residual layer (RL) formed during the night and contributes to the dispersion of volcanic CO_2. Accordingly, in the afternoon of June 2021 the average value of the wind speed was 0.23 m s^{-1}, that was lower than 0.36 m s^{-1} that was measured in the morning (Table 1).

The statistics from the $\delta^{13}C\text{-}CO_2$ data set collected during the October 2021 survey (Table 1) show differences compared to previous surveys. Figure 2d shows a distinct peak consistent with the $\delta^{13}C\text{-}CO_2$ of the standard air, as in the data set collected in August 2020 and the afternoon of June 2021. However, the $\delta^{13}C\text{-}CO_2$ data set shows a positive ending to less negative values, which is due to the local CO_2 source having a less ^{13}C-depleted isotopic signature. In addition, ∼85% of the measurements show values of CO_2 concentration in the range of 415–440 ppm vol (i.e., 747–792 mg m^{-3}) and ∼10% higher than 450 ppm vol (810 mg m^{-3}). Figure 3c shows selectively high CO_2 concentration values throughout the Vulcano Porto area. Several zones considered hazardous due to high CO_2 concentration were observed in Porto, Faraglione, Camping Sicilia, Piano delle Baracche and in the rural area of Discarica. The ^{13}C-depleted signature of CO_2 is expected to be conserved. The carbon isotopic signature of CO_2 produced from hydrocarbon combustion exhibits a typical ^{13}C-depleted carbon ($\delta^{13}C\text{-}CO_2$ from −30‰ to −40 ‰ vs. VPDB) either from combustion engines or electric power plant. In this case, the studies conducted on Vulcano would show a more depleted signature of CO_2 in the air in the case of pollution effects from hydrocarbon combustion. In contrast, the less ^{13}C-depleted CO_2 in air was detected by the pathway at Piano delle Baracche,

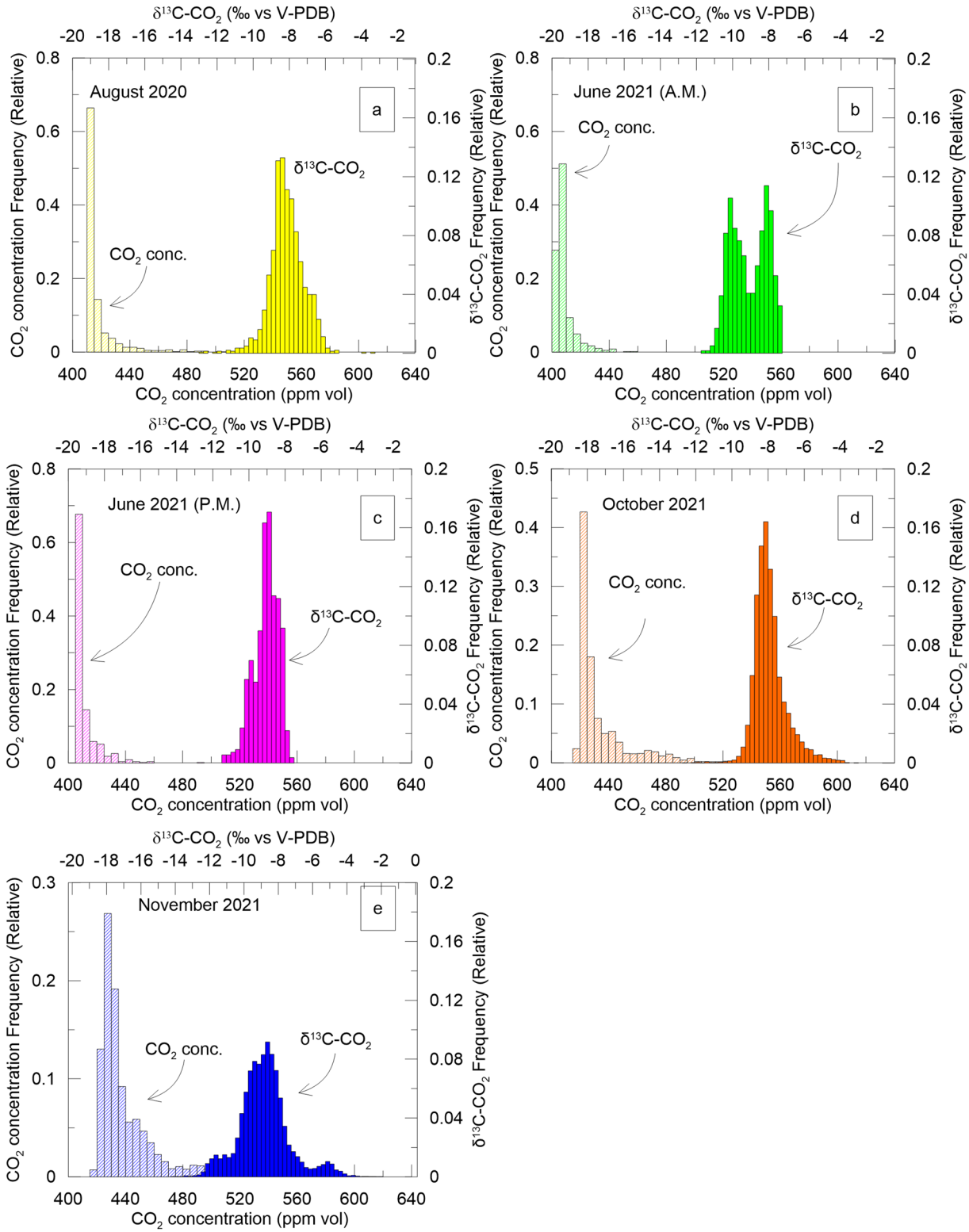

Figure 2. Statistics of $\delta^{13}C\text{-}CO_2$ and CO_2 concentration in air. Bottom horizontal axis shows values of CO_2 concentration; top horizontal axis refers to $\delta^{13}C\text{-}CO_2$. (a) $\delta^{13}C\text{-}CO_2$ (yellow filled bars) and CO_2 concentration in air (yellow dashed bars) measured on 5 August 2020 between 8:37 and 10:00 local time. (b) $\delta^{13}C\text{-}CO_2$ (green filled bars) and air CO_2 concentration (green dashed bars) measured on 16 June 2021 between 10:44 to 12:22 local time. (c) $\delta^{13}C\text{-}CO_2$ (purple filled bars) and CO_2 concentration (purple dashed bars) in air collected by meridian (i.e., from 17:53 to 19:24); (d) $\delta^{13}C\text{-}CO_2$ (orange filled bars) and air CO_2 concentration (orange dashed bars) measured on 19 October 2021 from 9:59 to 12:24; (e) $\delta^{13}C\text{-}CO_2$ (blue filled bars) and air CO_2 concentration (blue dashed bars) measured on 24 November 2021 from 9:19 to 12:31.

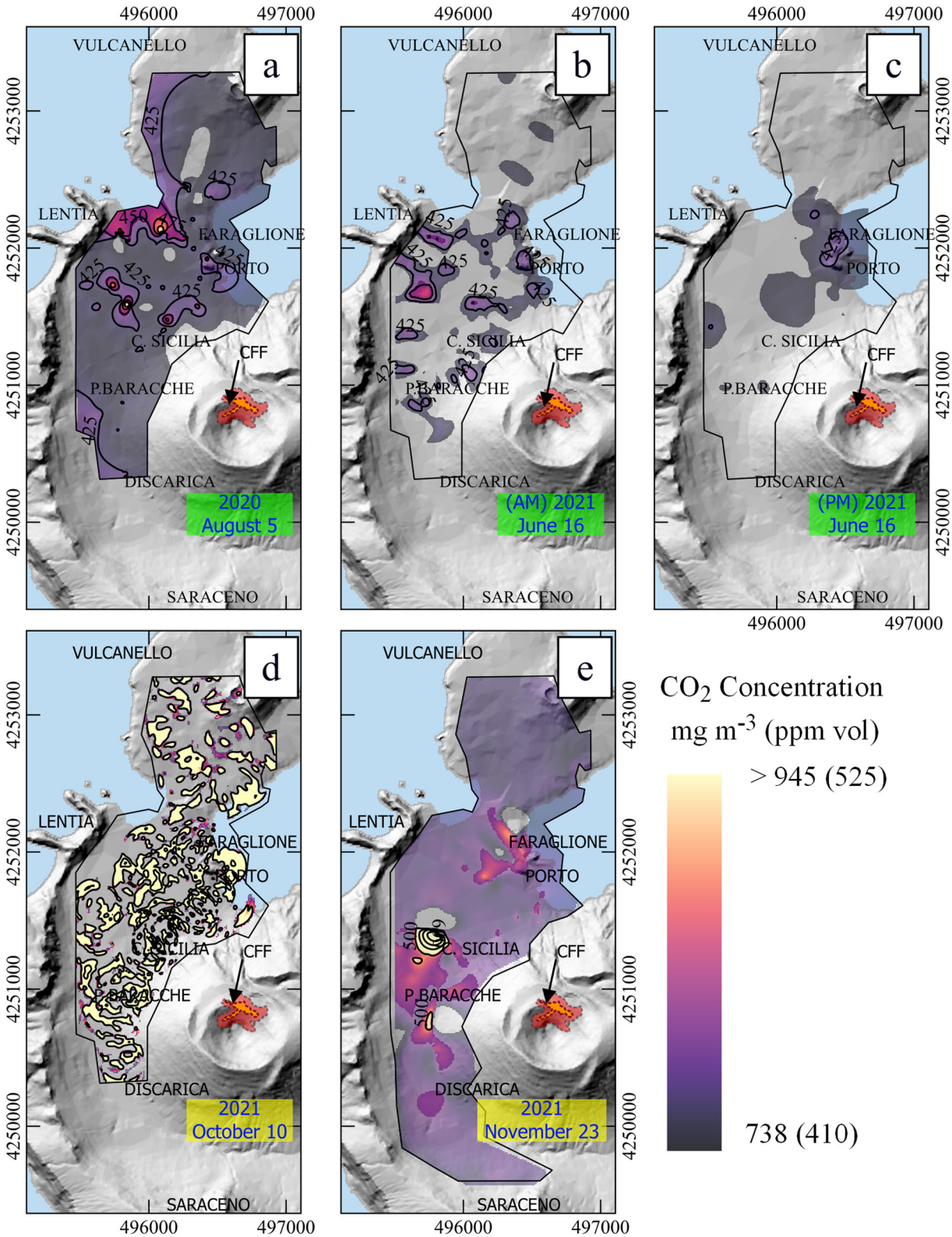

Figure 3. CO_2 concentration in the air at Vulcano, Italy. The limit of 380 ppm vol was used to achieve 100% transparency. Basemap DEM from Tinitaly (Tarquini et al., 2023) for all maps. (a) CO_2 concentration of air on 5 August 2020; (b) CO_2 concentration of air on 16 June 2021 (from 10:44 to 12:22 local time); (c) CO_2 concentration of air on 16 June 2021 (from 17:53 to 19:24 local time); (d) CO_2 concentration of air on 19 October 2021; (e) CO_2 concentration of air on 24 November 2021.

showing that the impact of the human-caused emissions during the period of the volcanic degassing crisis can be neglected. We conclude that CO_2 emissions from the ground mixed with CO_2 from the crater plume that fell through the flanks of the volcanic cone during the degassing crisis in 2021.

The local CO_2 source with a less ^{13}C-depleted isotopic signature persisted into November 2021. Figure 2e shows that $\delta^{13}C\text{-}CO_2$ has a small peak at $\delta^{13}C\text{-}CO_2 \approx -5‰$ and ~50% of the data set has $\delta^{13}C\text{-}CO_2$ values higher than the reference standard air. The data set collected in November 2021 shows the most abundant value consistent with $\delta^{13}C\text{-}CO_2 \approx -8‰$. Both the October and November 2021 datasets are characterized by high average CO_2 concentrations (Table 1). In November, ~98% of the concentration measurements showed values >420 ppm vol (756 mg m^{-3}) and ~10% were higher than 450 ppm vol (810 mg m^{-3}). From the south of Discarica to Vulcanello, CO_2 concentration was high everywhere and two sites with very high CO_2 concentration (>500 ppm vol) were located in the zone between Camping Sicilia and Piano delle Baracche and at Faraglione (Figure 3e).

Irregular and sudden spatial variations of $\delta^{13}C\text{-}CO_2$ in CO_2 of the air at Vulcano Porto distinguish the results of the surveys conducted in October and November 2021 (Figures 4d and 4e) from those of the August 2020 surveys (Figure 4a) and from the two surveys carried out on 16 June 2021 (Figures 4b and 4c). Figure 4a shows that CO_2 near the base of Mount Lentia ($\delta^{13}C\text{-}CO_2 = -6.8‰$) is less ^{13}C-depleted than standard air ($\delta^{13}C\text{-}CO_2 = -8.0‰$), while CO_2 in air NNW of the Faraglione zone, is more ^{13}C-depleted compared to CO_2 in standard air. On the morning of 16 June, spatial variations of $\delta^{13}C\text{-}CO_2$ in the air at Vulcano Porto show an almost NS elongated area with less ^{13}C-depleted values than the standard air. In the afternoon of the same day, measurement of the air CO_2 showed comparable $\delta^{13}C\text{-}CO_2$ values with those of standard air at Faraglione, while $\delta^{13}C\text{-}CO_2$ values in the entire Vulcano Porto zone were ^{13}C-poorer than those of standard air. The spatial variations of $\delta^{13}C\text{-}CO_2$ in October and November 2021 were different from those observed in June 2021 and August 2020. In particular, in October 2021, CO_2 in the air near Piano delle Baracche was less ^{13}C-depleted, and $\delta^{13}C\text{-}CO_2$ values were similar to those measured at Faraglione. This result suggests an isotopic forcing of CO_2 in the air due to volcanic degassing caused by a combination of increased CO_2 emissions from the soils and the dispersion of volcanic plume. The November 2021 spatial survey yielded a similar result, with measured $\delta^{13}C\text{-}CO_2$ values less depleted of ^{13}C (i.e., $\delta^{13}C\text{-}CO_2 = -6.5‰$) than standard air. In particular, the least ^{13}C-depleted values were measured in the area between Camping Sicilia and Mount Lentia. The latter represents an effective topographic barrier to air circulation within the La Fossa caldera.

In summary, a comparison between the statistics (Figure 2) and the spatial variations of the CO_2 content of the air at Vulcano Porto (Figure 3) shows that the CO_2 concentration has changed significantly in the period 2020 to 2021. The main changes were (a) the increase in CO_2 concentration in October 2021, (b) remarkable spatial variations in $\delta^{13}C\text{-}CO_2$ throughout the Vulcano Porto caldera (Figure 4), and (c) variations in CO_2 dispersion during the day on 16 June 2021.

4.2. $\delta^{18}O$ of the CO_2 in the Air

Figure 5 shows the statistics of $\delta^{18}O$ in air CO_2 during the five surveys conducted at Vulcano Porto (filled bars) compared to CO_2 concentration (dashed bars) from 2020 to 2021. Several variations in $\delta^{18}O\text{-}CO_2$ occurred during this time window, but the most significant change concerns the distribution of the data set collected in 2021.

Throughout the period of observation, the most common value was $\delta^{18}O\text{-}CO_2 = \sim -3‰$, indicating that the CO_2 content of the air on Vulcano was significantly ^{18}O-depleted compared to the CO_2 of the standard air in equilibrium with oceanic water (i.e., $\delta^{18}O = \sim -0.1‰$, Keeling, 1961). The distribution of the other values is almost symmetrical to the most abundant value.

Figure 5a shows that the $\delta^{18}O\text{-}CO_2$ value in 2020 has a smoothed, bifurcated distribution with two peaks that have similar abundance (i.e., ~0.08). Both the more ^{18}O-depleted peak (i.e., $\delta^{18}O\text{-}CO_2 \approx -4.0‰$) and the less ^{18}O-depleted peak (i.e., $\delta^{18}O\text{-}CO_2 \approx -1.0‰$) are more negative than the standard CO_2 in air at equilibrium with oceanic water. The negative ending tail of CO_2 depleted in ^{18}O suggests that volcanic CO_2 with $\delta^{18}O\text{-}CO_2 \approx -11.6‰$ (Capasso et al., 1997; Chiodini et al., 2000) affects the oxygen isotopic composition of CO_2 in air at Vulcano Porto. This result is consistent with the less ^{13}C-depleted CO_2 that the air at Vulcano had during the same survey. The other values show a relative peak at $\delta^{18}O\text{-}CO_2 \approx -1.3‰$ and a positive ending tail toward less ^{18}O-depleted values corresponding to CO_2 in the air in equilibrium with seawater.

A lower ^{18}O-depletion in CO_2 was observed in October 2021 (Figure 5d), when $\delta^{18}O\text{-}CO_2 \approx -1.5‰$ was the most common value. The data set shows a positive termination toward less ^{18}O-depleted values and some zones showed rather ^{18}O-enriched CO_2 (i.e., ~1% of the data set). A few positive values of $\delta^{18}O\text{-}CO_2$ (<1%) were measured

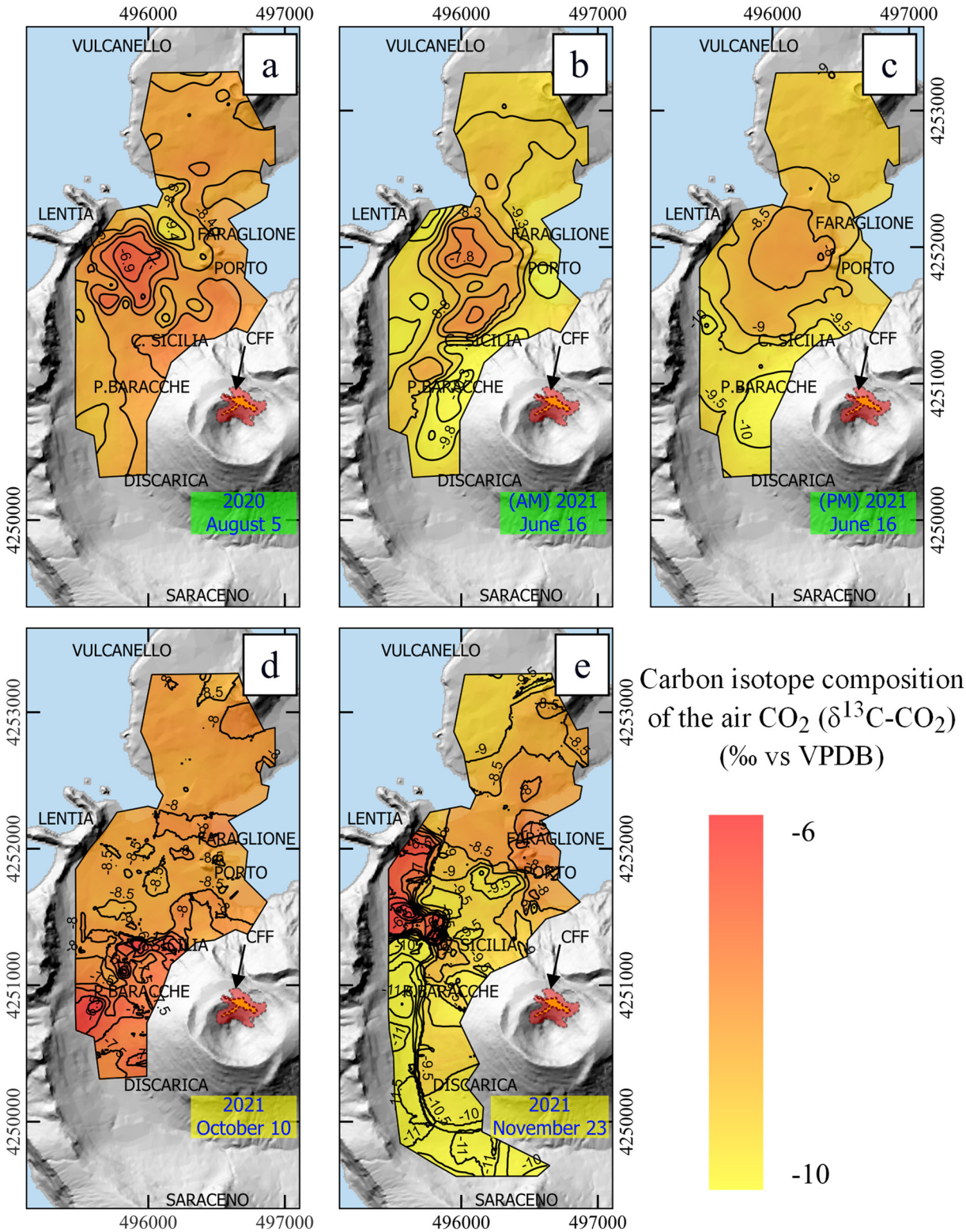

Figure 4. Spatial variations of $\delta^{13}C$-CO_2 through the pathway at Vulcano Porto, Italy. Basemap DEM from Tinitaly (Tarquini et al., 2023) for all maps. (a) $\delta^{13}C$-CO_2 in the air on 5 August 2020; (b) $\delta^{13}C$-CO_2 in the air on 16 June 2021 (from 10:44 to 12:22 local time); (c) $\delta^{13}C$-CO_2 in the air on 16 June 2021 (from 17:53 to 19:24 local time); (d) $\delta^{13}C$-CO_2 in the air on 19 October 2021; (e) $\delta^{13}C$-CO_2 in the air on 24 November 2021.

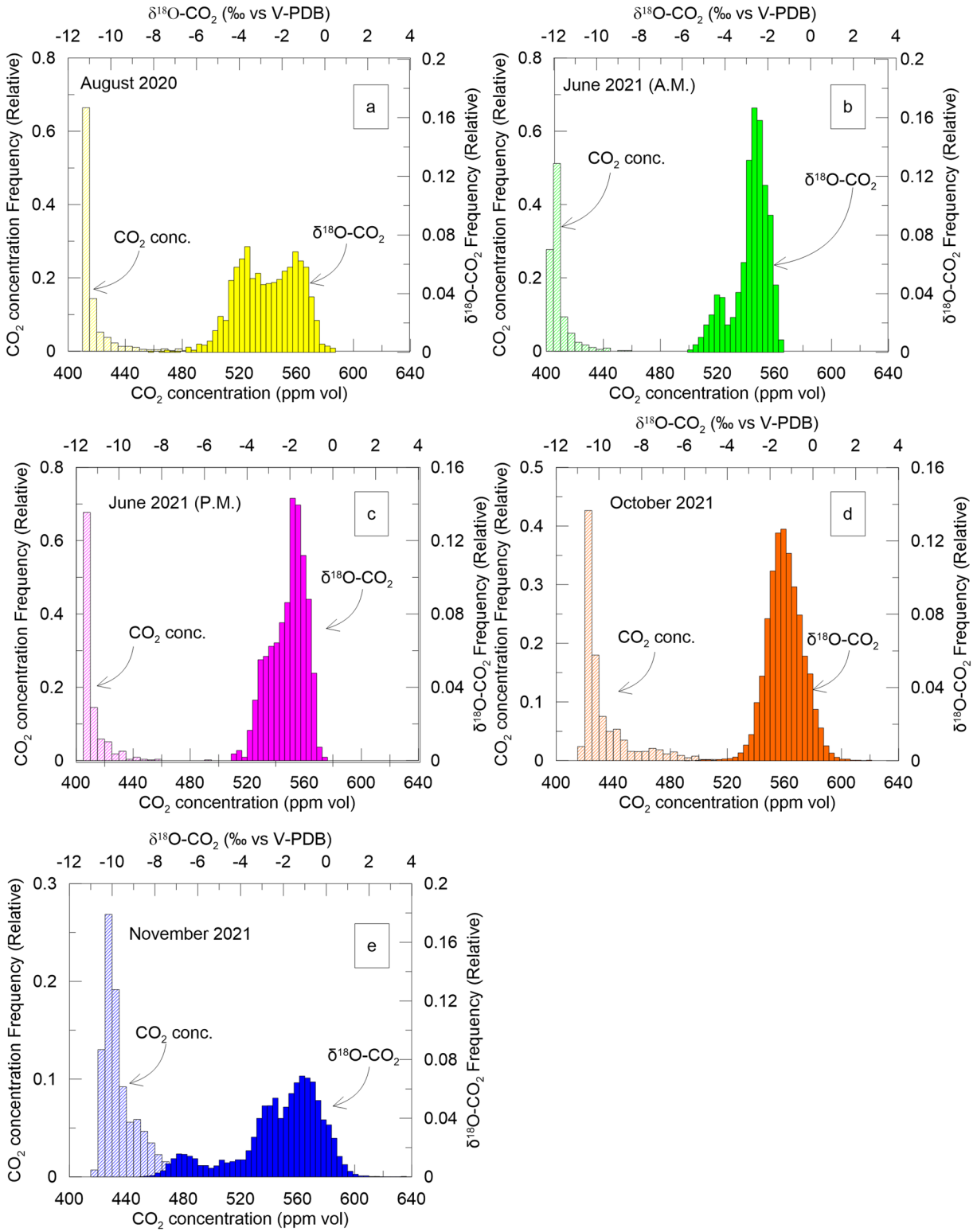

Figure 5. Statistics of $\delta^{18}O\text{-}CO_2$ and CO_2 concentration in air. Bottom horizontal axis shows values of CO_2 concentration; top horizontal axis refers to $\delta^{13}C\text{-}CO_2$. (a) $\delta^{18}O\text{-}CO_2$ (yellow filled bars) and CO_2 concentration in air (yellow dashed bars) measured on 5 August 2020 from 8:37 to 10:00 local time. (b) $\delta^{18}O\text{-}CO_2$ (green filled bars) and air CO_2 concentration (green dashed bars) measured on 16 June 2021 from 10:44 to 12:22. (c) $\delta^{18}O\text{-}CO_2$ (purple filled bars) and air CO_2 concentration (purple dashed bars) measured on 16 June 2021 by meridian (i.e., from 17:53 to 19:24); (d) $\delta^{18}O\text{-}CO_2$ (orange filled bars) and air CO_2 concentration (orange dashed bars) measured on 19 October 2021 from 9:59 to 12:24; (e) $\delta^{18}O\text{-}CO_2$ (blue filled bars) and air CO_2 concentration (i.e., blue dashed bars in Figure 4e) measured on 24 November 2021 from 9:19 to 12:31.

during the November 2021 survey, when the $\delta^{18}O\text{-}CO_2$ shows three peaks in the data distribution (Figure 5e). The most common value of $\delta^{18}O\text{-}CO_2$ for the less ^{18}O-depleted grouping corresponds to $\delta^{18}O\text{-}CO_2 \approx -1.0‰$, which is more ^{18}O-depleted than air CO_2 at equilibrium with ocean water (i.e., $\delta^{18}O\text{-}CO_2 \approx -0.1$ ‰), while the other two notable peaks are $\delta^{18}O\text{-}CO_2 \approx -2.5‰$ and $\delta^{18}O\text{-}CO_2 \approx -6.5‰$. This observation indicates that Figure 5b shows a negative termination of $\delta^{18}O\text{-}CO_2$ from −6.0 ‰ to −8.0 ‰, approaching the $\delta^{18}O$ values of volcanic CO_2. These subsets of measurements could have been affected to varying degrees by volcanic CO_2.

In summary, comparison of atmospheric CO_2 concentration and stable isotope composition statistics showed that the pattern of $\delta^{18}O\text{-}CO_2$ changed during the period from 2020 to 2021. The spatial variations of $\delta^{18}O\text{-}CO_2$ values along the Vulcano Porto route are shown in Figure 6. In the La Fossa caldera, some variations were observed during each survey, with strongest changes in $\delta^{18}O\text{-}CO_2$ in the time domain (Figures 6a–6e). The least depleted $\delta^{18}O$ values (i.e., $\delta^{18}O\text{-}CO_2 > -2.0$ ‰) were measured at Porto, Faraglione, and the eastern part of the target zone. The lowest $\delta^{18}O$ values (i.e., $\delta^{18}O\text{-}CO_2 < -4.0$ ‰) were observed at Vulcano Porto, Lentia, Discarica, and Saraceno. Smoothed spatial variations were observed on 5 August 2020, when CO_2 was at its least ^{18}O-depleted levels throughout the study area (Figure 6a). In June 2021, atmospheric CO_2 was less depleted in ^{18}O and the most negative $\delta^{18}O\text{-}CO_2$ values were measured near Lentia during the morning survey (Figure 6b). The $\delta^{18}O\text{-}CO_2$ showed fewer negative values during the afternoon (Figure 6c). The results of these two surveys illustrate the influence of photosynthesis on diurnal patterns of $\delta^{18}O\text{-}CO_2$ at Vulcano Porto. Due to plant discrimination of ^{18}O (Flanagan et al., 1997; Park & Epstein, 1960), less ^{18}O removal in atmospheric CO_2 occurs during photosynthesis. At night, when three leaves release CO_2, $\delta^{18}O\text{-}CO_2$ shift to ^{18}O-depleted values. A comparison between morning and afternoon $\delta^{18}O\text{-}CO_2$ values shows the effects of photosynthesis on the stable isotopic composition of CO_2 in the air. These results are consistent with an increase in the photosynthetic signal on airborne CO_2, which is consistent with an increase in net primary production in June 2021 compared to August 2020. Spatial variations of $\delta^{18}O\text{-}CO_2$ in October 2021 differed from those observed in previous surveys (Figure 6d). The less ^{18}O-depleted values were found at Vulcanello, Discarica, and Lentia, while the highest depletion of CO_2 in ^{18}O was measured at Porto (Figure 6d). The results of the survey conducted in November 2021 show similar lateral variations of $\delta^{18}O\text{-}CO_2$ as those observed in October 2021. The $\delta^{18}O\text{-}CO_2$ was less ^{18}O-poor in Faraglione and Porto, where the $\delta^{18}O\text{-}CO_2$ was similar or slightly ^{18}O-enriched compared to air CO_2 in equilibrium with seawater. Moreover, some remarkable differences are evident in November 2021 compared to October 2021. Indeed, the strongest ^{18}O-depletion of air CO_2 was observed at Piano delle Baracche, Camping Sicilia, Discarica, and Saraceno zones. As mentioned above, the oxygen fractionation of atmospheric CO_2 in the tree leaves occurs through photosynthesis. The distribution of vegetation on Vulcano is fairly homogeneous and no significant spatial variations in oxygen isotope fractionation are expected. Arguably, the observed variations are due to a local CO_2 source that has a distinct oxygen isotope signature. Variations in $\delta^{18}O\text{-}CO_2$ may also be due to changes in the hydrology of the regions, which could be plausible on a longer time scale (i.e., several weeks or several months). However, only a few hours are required for each survey, and the duration of the measurement can be considered instantaneous for all practical purposes. Therefore, the lateral variations of $\delta^{18}O\text{-}CO_2$ on Vulcano cannot be fully explained by photosynthetic effects.

5. Discussion

Several studies have pointed out the effects of volcanic emissions on the chemical composition of the atmosphere. This study aims to evaluate the effects of volcanic degassing on the concentration of CO_2 in the air at Vulcano Porto using stable isotopes in CO_2. The isotopic signature of volcanic CO_2 helps quantify the effects of variations in volcanic degassing on airborne CO_2 concentrations. Previous studies have observed a clear correspondence between local CO_2 source and airborne CO_2 through measurements of $\delta^{13}C\text{-}CO_2$ (Di Martino & Capasso, 2021; Di Martino & Gurrieri, 2022b), while $\delta^{18}O\text{-}CO_2$ has helped to assess CO_2 fractionation during transport from sources to sinks.

5.1. Source of the Air CO_2

The Keeling plot approach helps investigate the predominant source of CO_2 in the air by using $\delta^{13}C\text{-}CO_2$ versus the reciprocal of CO_2 concentration (Keeling, 1958). This approach results from the mass balance when a local CO_2 source increases the concentration from the atmospheric background. The mathematical formulation of this model includes the following equations:

$$C_m = C_a + C_s \quad (1)$$

and

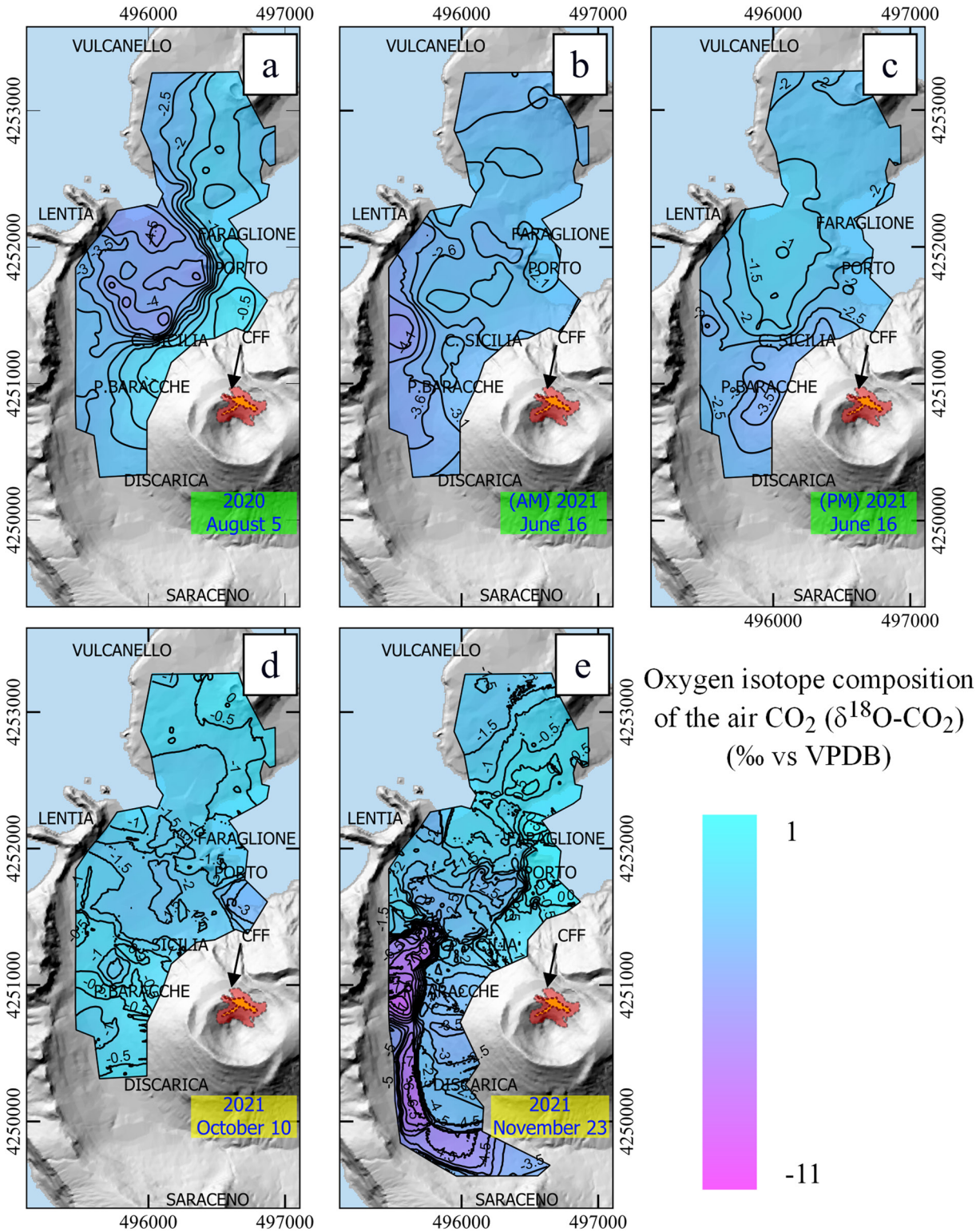

Figure 6. Spatial variations of $\delta^{18}O$–CO_2 through the pathway at Vulcano Porto. Basemap DEM from Tinitaly (Tarquini et al., 2023) for all maps. (a) $\delta^{18}O$–CO_2 measured on 5 August 2020 from 8:37 to 10:00 local time. (b) $\delta^{18}O$–CO_2 measured on 16 June 2021 from 10:44 to 12:22; (c) $\delta^{18}O$–CO_2 from 17:53 to 19:24, (d) $\delta^{18}O$–CO_2 measured on 19 October from 9:59 to 12:24; (e) $\delta^{18}O$–CO_2 measured on 24 November 2021 from 9:19 to 12:31.

$$\delta^{13}C_m \cdot C_m = \delta^{13}C_a \cdot C_a + \delta^{13}C_s \cdot C_s \quad (2)$$

where C and $\delta^{13}C$ are the CO_2 concentration and the $\delta^{13}C$-CO_2, respectively. The indices m, a, and s refer to the measured values, atmospheric background, and local source, respectively.

The linear combination of the above equation yields a straight line in the $\delta^{13}C$ versus 1/C plot (Keeling, 1958; Pataki et al., 2003), which has the following equation:

$$\delta^{13}C_m = \frac{C_a}{C_m}\left(\delta^{13}C_a - \delta^{13}C_s\right) + \delta^{13}C_s \quad (3)$$

Equation 3 provides the carbon isotope composition of the local CO_2 source when both the background and CO_2 sources are constant throughout the observation period. Figure 7 shows the Keeling plots of the data set collected in five surveys. The straight lines in this diagram represent the mixing between current atmospheric CO_2 and CO_2 from several local sources (Table S2 in Supporting Information S1), such as volcanic CO_2 from gas plumes (i.e., $\delta^{13}C$-$CO_2 = -0.2‰$ at Vulcano; Capasso et al., 1997; Chiodini et al., 1998), soil respired CO_2 at Vulcano Porto (average value at Vulcano Porto $\delta^{13}C$-$CO_2 = -15‰$; Di Martino & Gurrieri, 2022a, 2022b; Di Martino, Camarda, et al., 2016; Di Martino, Capasso, & Camarda, 2016; Di Martino et al., 2020), and human-related CO_2 (average values of CO_2 from fossil fuel combustion in Palermo, which can be considered representative of Sicily and the Aeolian Islands, are $\delta^{13}C$-$CO_2 = -39‰$; according to Di Martino & Gurrieri, 2022a, 2022b).

The different CO_2 sources have different carbon isotope signatures and form mixing lines with the local background, each with a specific slope (i.e., CO_2 from natural gas combustion, fossil fuel combustion, soil respiration, volcanic plume, and atmosphere-ocean interaction). CO_2 concentration shows a linear correlation with $\delta^{13}C$-CO_2, while the slopes of the straight lines varied over time. In August 2020 (Figure 7a) and June 2021 (Figures 7b and 7c), CO_2 concentration shows normalized values (i.e., against Holocene pre-industrial background $CO_2 = 684$ mg m^{-3}, corresponding to 348 ppm vol, according to Clark-Thorne & Yapp, 2003) in the range of 0.65–0.95, which was narrower than the range measured in October 2021 (Figure 7d) and November 2021 (Figure 7e). In addition, the data set collected during the morning survey in June 2021 has a wider range than the CO_2 concentration observed in the afternoon of the same day. Figure 7 clearly shows that the spatial variations of CO_2 in the air on Vulcano have several causes, including soil respiration and human-related CO_2 production from fossil fuel combustion. Sporadically, CO_2 concentrations in the air rise significantly (i.e., >30%) above background levels due to these gas sources. An increase in CO_2 production caused either by the influx of tourists to the island of Vulcano (i.e., during the summer months) or by the combustion of hydrocarbons to heat houses may be responsible for these fluctuations. Notable changes occurred in 2021, when the less ^{13}C-depleted signature of CO_2 in the air clearly shows that the increase in CO_2 concentration correlates with a resumption of volcanic degassing (Aiuppa et al., 2022; Di Martino et al., 2022; Federico et al., 2023; Inguaggiato et al., 2022). During this period, there was a remarkable increase in CO_2 concentration due to plume dispersion and φCO_2.

5.2. Estimation of the Volcanic CO_2 in the Air

An appropriate mass balance model for CO_2 in air includes both isotopic variables and concentration. Using literature values for $\delta^{13}C$-CO_2 and $\delta^{18}O$-CO_2 of standard air (i.e., $\delta^{13}C$-$CO_2 = -8‰$ and $\delta^{18}O$-$CO_2 = -0.1‰$ Keeling, 1961) and those of CO_2 from volcanic origin on Vulcano (i.e., $\delta^{13}C$-$CO_2 = -0.2‰$, $\delta^{18}O$-$CO_2 = -11.6‰$; Capasso et al., 1997; Chiodini et al., 1998), an isotopic mass balance model includes four unknowns (i.e., background air CO_2 concentration, CO_2 concentration in the volcanic plume, air CO_2 mixing fraction and volcanic CO_2 mixing fraction). The model consists of the following equation for the CO_2 concentration in the air

$$C_m = X_a \cdot C_a + X_V \cdot C_V \quad (4)$$

where C is the CO_2 concentration and X the mixing fraction between volcanic and air CO_2; the indices m, a, and V refer to measured, background and local volcanic CO_2 sources, respectively. In this model, we assume that (a) volcanic degassing significantly increases the CO_2 concentration relative to background and (b) volcanic emissions are the dominant local source of CO_2, at least during a crisis. According to the last assumption, the binary mixing equation for the relative weights of CO_2 from volcano and from the air is as follows:

$$X_a + X_V = 1 \quad (5)$$

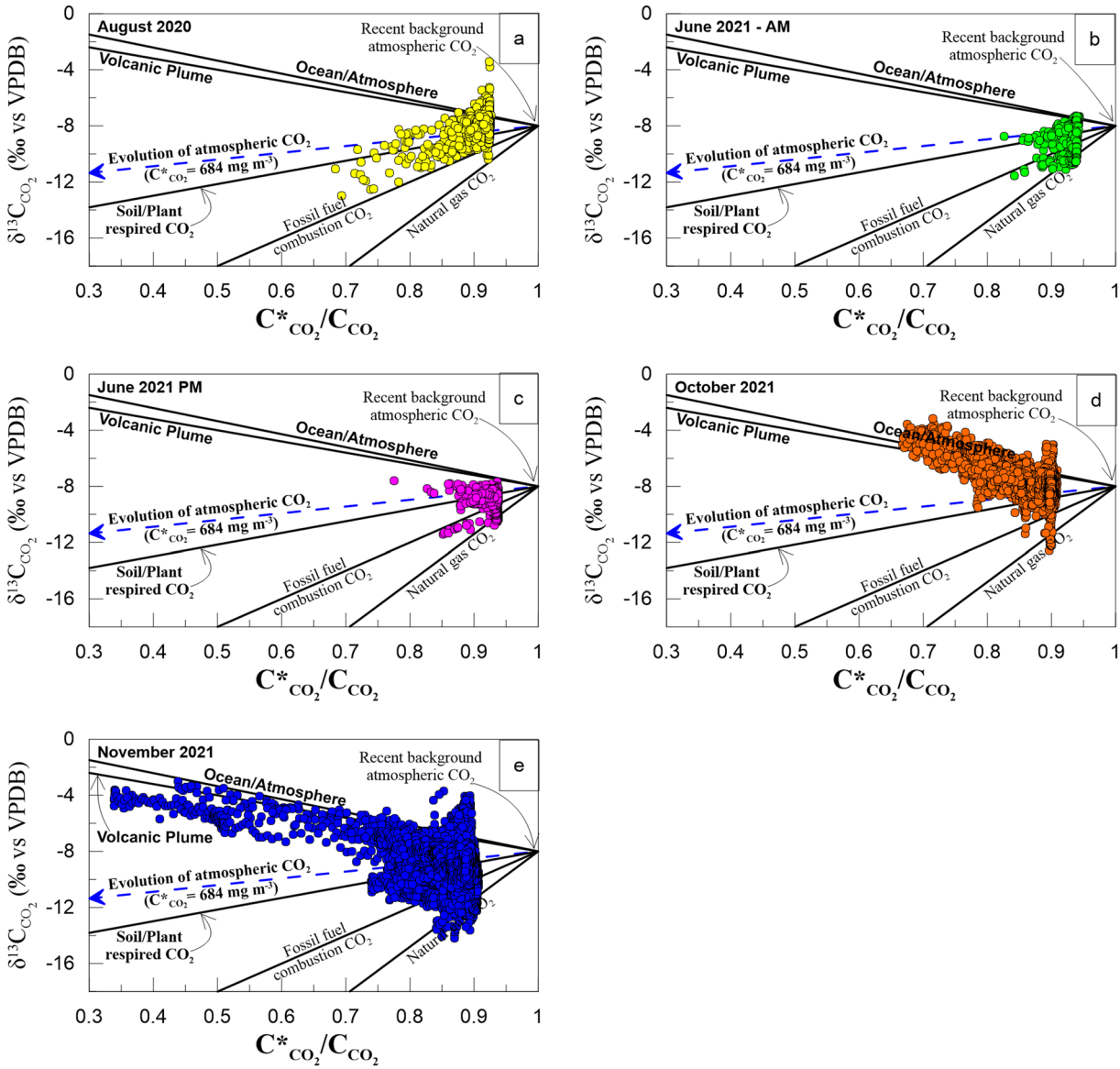

Figure 7. Carbon isotope composition of CO_2 in air vs. CO_2 concentration. The black lines are theoretical mixing lines that mix background air CO_2 in various proportions with various local CO_2 sources. The blue dashed line shows the current evolution of δ^{13}C-CO_2 assuming the Holocene growth rate of atmospheric CO_2. (a) August 2020 data set (yellow circle), (b and c) June 2021 data set from 9:59 to 12:24 and from 9:59 to 12:24, respectively; (d) October 2021 data set; (e) November 2021 data set. CO_2 concentration value was normalized using the atmospheric CO_2 reference concentration (i.e., Holocene background atmospheric CO_2 is 348 ppm vol ≈ 684 mg m^{-3} according to Clark-Thorne & Yapp, 2003).

Similarly, the following equations describe the isotopic mass balance model for carbon

$$\delta^{13}C_m \cdot C_m = \delta^{13}C_a \cdot C_a \cdot X_a + \delta^{13}C_V \cdot C_V \cdot X_V \quad (6)$$

and oxygen of CO_2

$$\delta^{18}O_m \cdot C_m = \delta^{18}O_a \cdot C_a \cdot X_a + \delta^{18}O_V \cdot C_V \cdot X_V \quad (7)$$

where δ^{13}C and δ^{18}O are the δ^{13}C-CO_2, δ^{18}O-CO_2, respectively. A combination of Equation 5 and 6 provides:

$$X_a = \frac{C_m \cdot \delta^{13}C_m - C_V \cdot \delta^{13}C_V \cdot X_V}{C_a \cdot \delta^{13}C_a} \quad (8)$$

Using Equation 8 in Equation 7 provides:

$$X_V = \frac{C_m}{C_V} \frac{\left(\delta^{18}O_m \cdot \delta^{13}C_a - \delta^{13}C_m \cdot \delta^{18}O_a\right)}{\left(\delta^{18}O_V \cdot \delta^{13}C_a - \delta^{13}C_V \cdot \delta^{18}O_a\right)} \tag{9}$$

Using both Equations 8 and 9 and rearranging Equation 4, we obtain

$$C_V \frac{C_a \cdot C_m \cdot \left(\delta^{18}O_m \cdot \delta^{13}C_a - \delta^{13}C_m \cdot \delta^{18}O_a\right)}{(C_m - C_a) \cdot (\delta^{18}O_V \cdot \delta^{13}C_a - \delta^{13}C_V \cdot \delta^{18}O_a) + C_m(\delta^{18}O_m \cdot \delta^{13}C_a - \delta^{13}C_m \cdot \delta^{18}O_a)} \tag{10}$$

which provides the concentration of volcanic CO_2 in the air (i.e., C_V).

Equation 10 allows the calculation of the volcanic CO_2 in the air using the measurements of CO_2 concentration, δ^{13}C-CO_2, δ^{18}O-CO_2 in the air at Vulcano. C_V indicates the CO_2 concentration of volcanic origin, which is above the local background concentration of CO_2 in the air.

Figure 8 shows the spatial variations of volcanic CO_2 (expressed in mg m^{-3} using the conversion factor 1 ppm vol $\approx$ 1.8 mg m^{-3}) in the air from August 2020 to November 2021. In August 2020, a combination of the restricted morphology of the inner Caldera della Fossa (i.e., the part of the island where the village of Vulcano Porto is located) and relative atmospheric stability during the early morning hours established suitable conditions for volcanic CO_2 accumulation, although volcanic degassing was at a low level. Data processing shows that volcanic CO_2 dispersion also occurs in the zone of Vulcanello. A similar condition occurred in the early morning of June 2021 (Figure 8b), before air turbulence begins to disturb the RL formed during the night in the low atmospheric planetary boundary layer (PBL) at Vulcano. After sunrise, when the ground surface of the Vulcano Porto zone receives solar radiation, the albedo warms the air. When sufficient thermal energy has accumulated, the lower layer of the atmosphere rises and turbulent vertical currents disperse volcanic CO_2. Once solar radiation is added to the heat flux from the ground of this zone of the island and the regional wind pattern, volcanic CO_2 in the air of Vulcano Porto decreases. This pattern arguably continues into the night, and further studies are planned to investigate this conclusion in more detail.

Figure 8c shows the dispersion of volcanic CO_2 in the late afternoon to early evening, when the concentration of volcanic CO_2 < 100 mg m^{-3} can be observed on Levante beach and Faraglione. Several fumarolic emissions and a large mud pool occur in this zone (Figure 1), which is a clear sign of a shallow volcanic/hydrothermal system on Vulcano. The spatial variation of volcanic CO_2 shows remarkable differences on 10 October 2021 (Figure 8d), when the volcanic CO_2 was sighted throughout the village of Vulcano Porto and the concentration was high (i.e., >900 mg m^{-3}). During this period, volcanic degassing on Vulcano suddenly increased (Aiuppa et al., 2022; Di Martino et al., 2022; Federico et al., 2023). In particular, Figure 8d shows some zones with a high concentration of volcanic CO_2 (i.e., >900 mg m^{-3} above background) at Discarica, Camping Sicilia, Piano delle Baracche, and Faraglione. Consistent with these results, these zones are susceptible to gas hazards because the morphology promotes the accumulation of volcanic CO_2 from both the crater plume and local φCO_2. Some mofetes and anomalous φCO_2 occur in these zones when volcanic degassing increases (Di Martino et al., 2020). An example of this occurrence was recorded in 2018 and in 2021 (Di Martino et al., 2022). Early on, when renewed degassing began on Vulcano, access to some homes in Piano delle Baracche and Camping Sicilia was prevented. These results are consistent with previous gas hazard assessment studies on Vulcano, where high-risk zones were associated with restricted air circulation (Granieri et al., 2014). In addition, this study shows that a significant amount of volcanic CO_2 was also found on Vulcanello during the period of intense degassing (Figure 8d).

A similar situation was observed on 23 November 2021, when volcanic CO_2 in the air throughout the village of Vulcano Porto was >72 mg m^{-3} (Figure 8e). Spatial variations of volcanic CO_2 in the air were moderate, with exceptionally high values (i.e., ~900 mg m^{-3} above background) of volcanic CO_2 in a broad zone that included Camping Sicilia and Piano delle Baracche. One possible explanation is that the combination of anomalous φCO_2 during a period of enhanced volcanic degassing and lower air turbulence significantly affects the accumulation of CO_2 in the lower layer of the atmosphere. In addition, a high concentration of volcanic CO_2 was observed during the morning hours when air turbulence should be high due to stronger solar radiation. Under these conditions, the air turbulence should dilute the volcanic CO_2 and homogenize the CO_2 concentration in the air. The high turbulence favors the dispersion of CO_2 in the morning hours compared to the night, when the stability of the RL creates the most favorable conditions for the accumulation of volcanic CO_2 in the air. Injection of a large amount

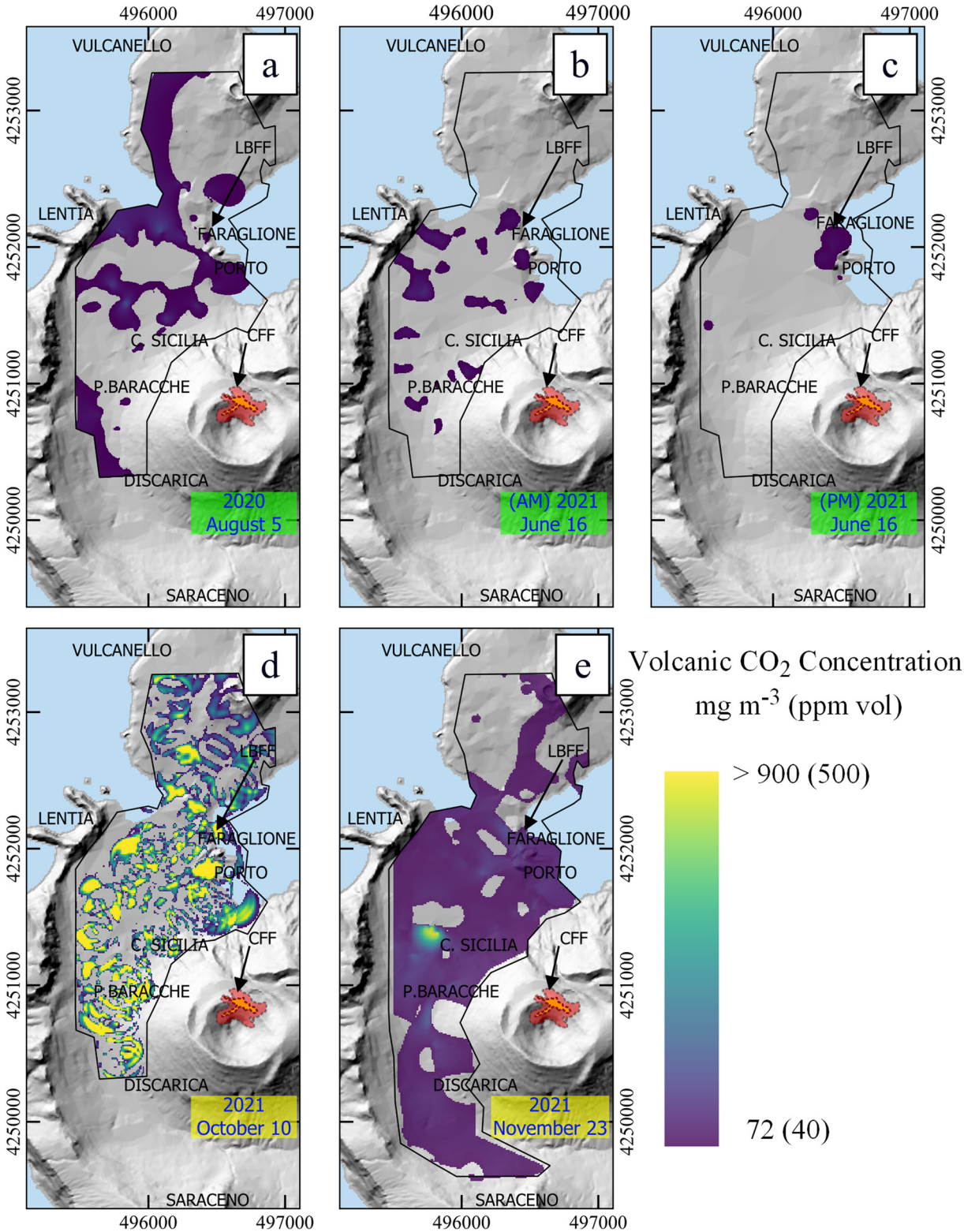

Figure 8. Results of the calculation of the concentration of volcanic CO_2 (mg m^{-3}) at Vulcano Porto according to Equation 10. A limit of 72 mg m^{-3} (40 ppm vol) volcanic CO_2 was used to achieve 100% transparency. Basemap DEM from Tinitaly (Tarquini et al., 2023) for all maps. CFF and LBFF indicate the position of the fumarolic fields at the crater rim and Levante beach, respectively. (a) Volcanic CO_2 concentration on 5 August 2020; (b) Volcanic CO_2 concentration on 16 June 2021 (from 10:44 to 12:22 local time); (c) Volcanic CO_2 concentration on 16 June 2021 (from 17:53 to 19:24 local time); (d) Volcanic CO_2 concentration on 10 October 2021; (e) Volcanic CO_2 concentration on 23 November 2021.

of volcanic CO_2 during the period of greater stability of the PBL (i.e., through plume dispersion or φCO_2 at night time) may result in high risks for residents sleeping in their homes at Vulcano Porto.

In summary, the isotopic composition of CO_2 in the air and data modeling based on mass balance show that volcanic CO_2 accumulation in the air results from a complex combination of several variables at Vulcano. First, injection of volcanic CO_2 alters both the concentration and isotopic signature of CO_2 in the air. The stability of the boundary layer during the night or arguably during periods of low wind speeds (Table 1) creates favorable conditions for an increase in CO_2 and the associated gas hazard. The spatial variations in the stable isotopic composition of CO_2 indicate that some zones are more susceptible to the gas hazard, that is, either zones with anomalous φCO_2 from depth or zones downwind of the gas plume. While zones of anomalous φCO_2 can be identified from measurements of soil CO_2 flux, the zones exposed to the effects of the volcanic gas plume are broader and can change depending on local wind direction and speed. Finally, the results of this study show that the stable isotopic composition of CO_2 in the air can help track the volcanic gas plume.

6. Conclusions

This study analyzed the effects of volcanic degassing on the spatial variations of CO_2 in the air and the main factors contributing to the dispersion of volcanic CO_2. The study of the stable isotopic composition of CO_2 in the air at Vulcano Porto showed irregular spatial variations of volcanic CO_2 in the air, suggesting that volcanic gas emissions may have different effects in different zones of Vulcano Porto.

The study of CO_2 in air is based on the spatial variations of $\delta^{13}C\text{-}CO_2$, $\delta^{18}O\text{-}CO_2$, and CO_2 concentration measured with a high-precision laser-based spectrophotometer (Delta Ray Thermo Scientific Instrument $\delta^{13}C\text{-}CO_2 = \pm 0.25$ ‰, $\delta^{18}O\text{-}CO_2 = \pm 0.25$ ‰, and CO_2 concentration $= \pm 1$ ppm vol, respectively). This instrument was installed in a car-based laboratory for data collection over a route through the village of Vulcano Porto. The results of five onsite measurements show that airborne CO_2 concentration varies due to several causes, including the gas emissions from the shallow volcanic/hydrothermal system at Faraglione, CO_2 generated by fossil fuel combustion, and the morphology of certain zones on the island of Vulcano.

In this study, an isotopic mass balance model was designed and developed to partition CO_2 between background air and volcanic CO_2. The model provides the concentration of volcanic CO_2 in the air (i.e., in either ppm vol or mg m^{-3}) to help quantify the effects of volcanic degassing on CO_2 in the air at Vulcano Porto.

A comparison of results collected in the morning and late afternoon of 16 June 2021 suggests that air turbulence due to reflection of solar radiation disturbs the stratification of air that forms in the PBL at night. Volcanic CO_2 remained in the air at Faraglione near a shallow hydrothermal mud pool in the late afternoon of 16 June. During the morning survey on 16 June, under conditions of volcanic degassing that can be considered identical to those of the afternoon, the stable isotopic signature of volcanic CO_2 was found in several zones of Vulcano Porto. A combination of causes, such as the high weight of CO_2 molecules and the low CO_2 diffusivity in the air, could explain the traces of nocturnal RL stability well into the morning. Further experimental studies are needed to fully understand the role of nocturnal RL and the extent of volcanic CO_2 injection, and to assess the effects of atmospheric stability on CO_2 dispersion and gas hazard.

Results obtained in 2020 and June 2021 provided a valuable guide for assessing the impact of increasing volcanic degassing that began in late summer 2021. On 10 October 2021, volcanic $CO_2 > 900$ mg m^{-3} was measured in several zones at Vulcano Porto. A larger amount of volcanic CO_2 was found at Faraglione, Camping Sicilia, Piano delle Baracche, and Discarica, where volcanic CO_2 emissions through the soil increased. Interestingly, the identification of volcanic CO_2 based on $\delta^{13}C\text{-}CO_2$, $\delta^{18}O\text{-}CO_2$, and CO_2 concentration shows that volcanic gas plume propagation can reach Vulcanello under unfavorable wind conditions (i.e., SE wind direction when Vulcanello is in the lee of the volcanic cone). The results of the 23 November survey show a high volcanic CO_2 content at Piano delle Baracche, while a lower volcanic CO_2 content was observed over Vulcano Porto compared to 10 October.

These results show that stable isotope measurements allow an assessment of the impact of volcanic degassing on airborne CO_2 concentrations and provide valuable results to identify zones more vulnerable to the gas hazard at Vulcano Porto. Volcanic risk mitigation includes specific actions aimed at increasing resilience by monitoring degassing activity. The resumption of volcanic degassing within a short period of time has never been recorded before at Vulcano, and it is important to understand how future plausible changes may increase the gas hazard in populated zones of Vulcano, as well as the risk of a volcanic explosion.

Data Availability Statement

The database of $\delta^{13}C\text{-}CO_2$, $\delta^{18}O\text{-}CO_2$, and the CO_2 concentration are from (https://doi.org/10.5281/zenodo.7013432). Cite as: Di Martino et al. (2022). Dataset of the air CO2 surveys performed at Vulcano from August 2020 to November 2021 [Dataset]. Zenodo. https://doi.org/10.5281/zenodo.7013432. Software that we used for data processing: Quantum GIS (https://www.qgis.org/it/site/).

Acknowledgments
The authors appreciated the valuable and deep comments from two anonymous Reviewers. The authors sincerely thank Dr Fabio Vita that kindly provided values of the wind speed reported in this study. We thank Dr Santina Messineo for her expert English revision. The Istituto Nazionale di Geofisica e Vulcanologia provided funding for Open Access publication in accordance with the CRUI-CARE agreement.

References

Aiuppa, A., Bitetto, M., Calabrese, S., Delle Donne, D., Lages, J., La Monica, F. P., et al. (2022). Mafic magma feeds degassing unrest at Vulcano Island, Italy. *Communications Earth & Environment*, *3*(1), 255. https://doi.org/10.1038/s43247-022-00589-1

Aiuppa, A., Fischer, T. P., Plank, T., & Bani, P. (2019). CO_2 flux emissions from the Earth's most actively degassing volcanoes, 2005–2015. *Scientific Reports*, *9*(1), 5442. https://doi.org/10.1038/s41598–019–41901–y

Andrew, R. M. (2018). Global CO_2 emissions from cement production, 1928–2017. *Earth System Data Science*, *10*(4), 2213–2239. https://doi.org/10.5194/essd–10–2213–2018

Badalamenti, B., Gurrieri, S., Hauser, S., Parello, F., & Valenza, M. (1988). Soil CO_2 output in the island of Vulcano during the period 1984–1988: Surveillance of gas hazard and volcanic activity. *Rendiconti della Societa Italiana di Mineralogia e Petrologia*, *43*, 893–899.

Badalamenti, B., Gurrieri, S., Hauser, S., Parello, F., & Valenza, M. (1991). Change in the soil CO_2 output at Vulcano during the summer 1998. *Acta Vulcanologica*, *1*, 219–221.

Barreca, G., Bruno, V., Cultrera, F., Mattia, M., Monaco, C., & Scarfì, L. (2014). New insights in the geodynamics of the Lipari–Vulcano area (Aeolian Archipelago, southern Italy) from geological, geodetic and seismological data. *Journal of Geodynamics*, *82*, 150–167. https://doi.org/10.1016/j.jog.2014.07.003

Behrenfeld, M. J., O'Malley, R. T., Siegel, D. A., McClain, C. R., Sarmiento, J. L., Feldman, G. C., et al. (2006). Climate–driven trends in contemporary ocean productivity. *Nature*, *444*(7120), 752–755. https://doi.org/10.1038/nature05317

Berner, R. A. (2003). The long–term carbon cycle, fossil fuels and atmospheric composition. *Nature*, *426*(6964), 323–326. https://doi.org/10.1038/nature02131

Bottinga, Y., & Craig, H. (1969). Oxygen isotope fractionation between CO_2 and water and isotopic composition of marine atmospheric CO_2. *Earth and Planetary Science Letters*, *5*(5), 285–295. https://doi.org/10.1016/s0012-821x(68)80054-8

Burton, M. R., Sawyer, G. M., & Granieri, D. (2013). Deep carbon emissions from volcanoes. *Reviews in Mineralogy and Geochemistry*, *75*(1), 323–354. https://doi.org/10.2138/rmg.2013.75.11

Calvert, J. G., Heywood, J. B., Sawyer, R. F., & Seinfeld, J. H. (1993). Achieving acceptable air quality: Some reflections on controlling vehicle emissions. *Science*, *261*(5117), 37–45. https://doi.org/10.1126/science.261.5117.37

Camarda, M., De Gregorio, S., Capasso, G., Di Martino, R. M. R., Gurrieri, S., & Prano, V. (2019). The monitoring of natural soil CO_2 emissions: Issue and perspectives. *Earth-Science Reviews*, *198*, 198–102928. https://doi.org/10.1016/j.earscirev.2019.102928

Camarda, M., De Gregorio, S., Di Martino, R. M. R., & Favara, R. (2016). Temporal and spatial correlations between soil CO_2 flux and crustal stress. *Journal of Geophysical Research: Solid Earth*, *121*(10), 7071–7085. https://doi.org/10.1002/2016JB013297

Camarda, M., De Gregorio, S., Di Martino, R. M. R., Favara, R., & Prano, V. (2020). Relationships between soil CO_2 flux and tectonic structures in SW Sicily. *Annales Geophysicae*, *63*. https://doi.org/10.4401/ag–8264

Camarda, M., Gurrieri, S., Di Martino, R. M. R., & Francofonte, V. (2023). *The combined surveying of soil CO_2 flux and air CO_2 concentration for gas hazard mitigation at Vulcano, Italy*. EGU General Assembly 2023. 24–28 Apr 2023, EGU23-16440. https://doi.org/10.5194/egusphere-egu23-16440

Camarda, M., Gurrieri, S., & Valenza, M. (2006a). CO_2 flux measurements in volcanic areas using the dynamic concentration method: Influence of soil permeability. *Journal of Geophysical Research*, *111*(B5), B05202. https://doi.org/10.1029/2005JB003898

Camarda, M., Gurrieri, S., & Valenza, M. (2006b). In situ permeability measurements based on a radial gas advection model: Relationships between soil permeability and diffuse CO_2 degassing in volcanic areas. *Pure and Applied Geophysics*, *163*(4), 897–914. https://doi.org/10.1007/s00024-006-0045-y

Capasso, G., Di Martino, R. M. R., Camarda, M., & Prano, V. (2017). Dissolved carbon in groundwater versus gas emissions from the soil: The two sides of the same coin. *Procedia Earth and Planetary Sciences*, *17*, 16–119. https://doi.org/10.1016/j.proeps.2016.12.021

Capasso, G., Di Martino, R. M. R., Caracausi, A., & Favara, R. (2019). Isotope determination of carbon and oxygen of CO_2 in natural and atmospheric gases using laser–based analyzer. Miscellanea INGV 49. In *15th international conference on gas geochemistry—ICGG15*. ISSN 1590–2595.

Capasso, G., Di Martino, R. M. R., Caracausi, A., & Favara, R. (2021). *Distinguishing human related, biological and geological carbon dioxide in the air through isotopic surveying*. European Geoscience Union General Assembly. EGU21–9620. https://doi.org/10.5194/egusphere–egu21–9620

Capasso, G., Favara, R., & Inguaggiato, S. (1997). Chemical features and isotopic composition of gaseous manifestations on Vulcano Island (Aeolian Islands Italy): An interpretative model of fluid circulation. *Geochimica et Cosmochimica Acta*, *61*(16), 3425–3440. https://doi.org/10.1016/s0016-7037(97)00163-4

Carapezza, M. L., Barberi, F., Ranaldi, M., Ricci, T., Tarchini, L., Barrancos, J., et al. (2011). Diffuse CO_2 soil degassing and CO_2 and H_2S concentrations in air and related hazards at Vulcano Island (Aeolian arc Italy). *Journal of Volcanology and Geothermal Research*, *207*(3–4), 130–144. https://doi.org/10.1016/j.jvolgeores.2011.06.010

Carapezza, M. L., & Federico, C. (2000). The contribution of fluid geochemistry to the volcano monitoring of Stromboli. *Journal of Volcanology and Geothermal Research*, *95*(1–4), 227–245. https://doi.org/10.1016/S0377–0273(99)00128–6

Chiarabba, C., De Gori, P., & Speranza, F. (2008). The southern Tyrrhenian subduction zone: Deep geometry, magmatism and Plio–Pleistocene evolution. *Earth and Planetary Science Letters*, *268*(3–4), 3–4. https://doi.org/10.1016/j.epsl.2008.01.036

Chiodini, G., Allard, P., Caliro, S., & Parello, F. (2000). ^{18}O exchange between steam and carbon dioxide in volcanic and hydrothermal gases: Implications for the source of water. *Geochimica et Cosmochimica Acta*, *64*, 14–2488. https://doi.org/10.1016/S0016–7037(99)00445–7

Chiodini, G., Cioni, R., Guidi, M., & Marini, L. (1991). Geochemical variations at Fossa Grande crater fumaroles (Vulcano Island, Italy) in summer 1988. *Acta Vulcanologica*, *1*, 179–192.

Chiodini, G., Cioni, R., Guidi, M., Marini, L., & Raco, B. (1998). Soil CO_2 flux measurements in volcanic and geothermal areas. *Applied Geochemistry*, *13*(5), 543–552. https://doi.org/10.1016/S0883–2927(97)00076–0

Chiodini, G., Frondini, F., & Raco, B. (1996). Diffuse emission of CO_2 from the Fossa crater, Vulcano Island (Italy). *Bulletin of Volcanology*, *58*(1), 41–50. https://doi.org/10.1007/s004450050124

Ciais, P., & Meijer, H. A. J. (1998). The $^{18}O/^{16}O$ isotope ratio of atmospheric CO_2 and its role in global carbon cycle research. In H. Griffiths (Ed.), *Stable isotope—Integration of biological, ecological and geochemical processes* (pp. 409–431). BIOS Scientific Publishers.

Clark-Thorne, S. T., & Yapp, C. J. (2003). Stable carbon isotope constraints on mixing and mass balance of CO_2 in an urban atmosphere: Dallas metropolitan area, Texas, USA. *Applied Geochemistry*, *18*(1), 75–95. https://doi.org/10.1016/S0883-2927(02)00054-9

De Astis, G., Lucchi, F., Dellino, P., La Volpe, L., Tranne, C. A., Frezzotti, M. L., & Peccerillo, A. (2013). Geology, volcanic history and petrology of Vulcano (central Aeolian Archipelago). In F. Lucchi, A. Peccerillo, J. Keller, C. A. Tranne, & P. L. Rossi (Eds.), *The Aeolian islands volcanoes* (Vol. 37, pp. 281–348). Geological Society.

De Astis, G., Ventura, G., & Vilardo, G. (2003). Geodynamic significance of the Aeolian volcanism (Southern Tyrrhenian Sea, Italy) in light of structural, seismological and geochemical data. *Tectonics*, *22*(4), 1040. https://doi.org/10.1029/2003TC001506

Diliberto, I. S., Gurrieri, S., & Valenza, M. (2002). Relationships between diffuse CO_2 emissions and volcanic activity on the island of Vulcano (Aeolian Islands Italy) during the period 1984–1994. *Bulletin of Volcanology*, *64*(3–4), 219–228. https://doi.org/10.1007/s00445-001-0198-6

Di Martino, R. M. R., Camarda, M., Capasso, G., Gurrieri, S., & Prano, V. (2022). Soil CO_2 flux surveys during 2021 at Vulcano—Aeolian Island, Italy. Cities on Volcanoes.

Di Martino, R. M. R., Camarda, M., & Gurrieri, S. (2021). Continuous monitoring of hydrogen and carbon dioxide at Stromboli volcano (Aeolian Islands, Italy). *The Italian Journal of Geosciences*, *141*(1), 79–94. https://doi.org/10.3301/IJG.2020.26

Di Martino, R. M. R., Camarda, M., Gurrieri, S., & Valenza, M. (2013). Continuous monitoring of hydrogen and carbon dioxide at Mt Etna. *Chemical Geology*, *357*, 41–51. https://doi.org/10.1016/j.chemgeo.2013.08.023

Di Martino, R. M. R., Camarda, M., Gurrieri, S., & Valenza, M. (2016). Asynchronous changes of CO_2, H_2, and He concentrations in soil gases: A theoretical model and experimental results. *Journal of Geophysical Research: Solid Earth*, *121*(3), 1565–1583. https://doi.org/10.1002/2015JB012600

Di Martino, R. M. R., & Capasso, G. (2019). Fast and accurate both carbon and oxygen isotope determination in volcanic and urban gases using laser–based analyzer. *Geophysical Research Abstracts*, *21*, 5095.

Di Martino, R. M. R., & Capasso, G. (2021). On the complexity of anthropogenic and geological sources of carbon dioxide: Onsite differentiation using isotope surveying. *Atmospheric Environment*, *2556*, 118446. https://doi.org/10.1016/j.atmosenv.2021.118446

Di Martino, R. M. R., Capasso, G., & Camarda, M. (2016). Spatial domain analysis of carbon dioxide from soils on Vulcano Island: Implications for CO_2 output evaluation. *Chemical Geology*, *444*, 59–70. https://doi.org/10.1016/j.chemgeo.2016.09.037

Di Martino, R. M. R., Capasso, G., Camarda, M., De Gregorio, S., & Prano, V. (2020). Deep CO_2 release revealed by stable isotope and diffuse degassing surveys at Vulcano (Aeolian Islands) in 2015–2018. *Journal of Volcanology and Geothermal Research*, *401*, 106972. https://doi.org/10.1016/j.jvolgeores.2020.106972

Di Martino, R. M. R., & Gurrieri, S. (2022a). Dataset of the air CO_2 surveys performed at Vulcano from August 2020 to November 2021 [Dataset]. Zenodo. https://doi.org/10.5281/zenodo.7013432

Di Martino, R. M. R., & Gurrieri, S. (2022b). Theoretical principles and application to measure the flux of carbon dioxide in the air of urban zones. *Atmospheric Environment*, *288*(4), 119302. https://doi.org/10.1016/j.atmosenv.2022.119302

Di Martino, R. M. R., & Gurrieri, S. (2023). *Stable isotope surveys reveal variations in the air CO_2 during the unrest event at Vulcano, Italy, in 2021*. EGU General Assembly 2023. 24–28 Apr 2023, EGU23-11463. https://doi.org/10.5194/egusphere-egu23-11463

Di Martino, R. M. R., Gurrieri, S., Diliberto, I. S., Vita, F., Camarda, M., Francofonte, V., et al. (2021b). Gas emissions in volcanic islands: Establishing an early warning network for gas hazard management. *EGU General Assembly*. online, 19–30 Apr 2021, EGU21–8422. https://doi.org/10.5194/egusphere–egu21–8422

Federico, C., Cocina, O., Gambino, S., Paonita, A., Branca, S., Coltelli, M., et al. (2023). Inferences on the 2021 ongoing volcanic unrest at Vulcano Island (Italy) through a comprehensive multidisciplinary surveillance network. *Remote Sensing*, *15*(5), 1405. https://doi.org/10.3390/rs15051405

Flanagan, L. B., Brooks, J. R., Vanery, G. T., & Ehleringr, J. R. (1997). Discrimination against $C^{18}O^{16}O$ during photosynthesis and the oxygen isotope ratio of respired CO_2 in boreal forest ecosystems. *Global Biogeochemical Cycles*, *11*(1), 83–98. https://doi.org/10.1029/96gb03941

Forni, F., Lucchi, F., Peccerillo, A., Tranne, C. A., Rossi, P. L., & Frezzotti, M. L. (2013). Stratigraphy and geological evolution of the Lipari volcanic complex (central Aeolian archipelago). In F. Lucchi, A. Peccerillo, J. Keller, C. A. Tranne, & P. L. Rossi (Eds.), *The Aeolian islands volcanoes* (Vol. 37, pp. 213–279). Geological Society.

Giorgi, F., Coppola, E., & Raffaele, F. (2018). Threatening levels of cumulative stress due to hydroclimatic extremes in the 21st century. *Npj Climate and Atmospheric Science*, *1*, 18. https://doi.org/10.1038/s41612–018–0028–6

Giorgi, F., Im, E. S., Coppola, E., Diffenbaugh, N. S., Gao, X. J., Mariotti, L., & Shi, Y. (2011). Higher hydroclimatic intensity with global warming. *Journal of Climate*, *24*(20), 5309–5324. https://doi.org/10.1175/2011JCLI3979.1

Granieri, D., Carapezza, M. L., Barberi, F., Ranaldi, M., Ricci, T., & Tarchini, L. (2014). Atmospheric dispersion of natural carbon dioxide emissions on Vulcano Island, Italy. *Journal of Geophysical Research: Solid Earth*, *119*(7), 5398–5413. https://doi.org/10.1002/2013JB010688

Granieri, D., Carapezza, M. L., Chiodini, G., Avino, R., Caliro, S., Ranaldi, M., et al. (2006). Correlated increase in CO_2 fumarolic content and diffuse emission from La Fossa crater (Vulcano, Italy): Evidence of volcanic unrest or increasing gas release from a stationary deep magma body? *Geophysical Research Letters*, *33*(13), L13316. https://doi.org/10.1029/2006GL026460

Gurrieri, S., Di Martino, R. M. R., Camarda, M., & Francofonte, V. (2022). Continuous monitoring of soil CO_2 flux and air CO_2 concentration at Vulcano during 2021. In *Abstract Volume 5 Conferenza A. RITTMANN, Catania 29 September 1st October 2022*, O. Cocina, C. Tranne, A. Vona, & M. Viccaro (Eds). *Miscellanea INGV* (Vol. 70, p. 1340). https://doi.org/10.13127/misc/70

Gurrieri, S., Liuzzo, M., & Giudice, G. (2008). Continuous monitoring of soil CO_2 flux on Mt. Etna: The 2004–2005 eruption and the role of regional tectonics and volcano tectonics. *Journal of Geophysical Research: Solid Earth*, *113*, B9. https://doi.org/10.1029/2007JB005003

Gurrieri, S., Liuzzo, M., Giuffrida, G., & Boudoire, G. (2021). The first observations of CO_2 and CO_2/SO_2 degassing variations recorded at Mt. Etna during the 2018 eruptions followed by three strong earthquakes. *The Italian Journal of Geosciences*, *140*, 1–106. https://doi.org/10.3301/IJG.2020.25

Harries, J. E., Brindley, H. E., Sagoo, P. J., & Bantges, R. J. (2001). Increases in greenhouse forcing inferred from the outgoing longwave radiation spectra of the Earth in 1970 and 1997. *Nature*, *410*(6826), 355–357. https://doi.org/10.1038/35066553

Hasanbeigi, A., Price, L., & Lin, E. (2012). Emerging energy–efficiency and CO_2 emission–reduction technologies for cement and concrete production: A technical review. *Renewable and Sustainable Energy Reviews*, *16*(8), 6220–6238. https://doi.org/10.1016/j.rser.2012.07.019

Hennessy, K. J., Gregory, J. M., & Mitchell, J. F. B. (1997). Changes in daily precipitation under enhanced greenhouse conditions. *Climate Dynamics*, *13*(9), 667–680. https://doi.org/10.1007/s003820050189

Inguaggiato, S., Vita, F., Diliberto, I. S., Inguaggiato, C., Mazot, A., Cangemi, M., & Corrao, M. (2022). The volcanic activity changes occurred in the 2021–2022 at Vulcano island (Italy), inferred by the abrupt variations of soil CO_2 output. *Scientific Reports*, *12*(1). https://doi.org/10.1038/s41598-022-25435-4

Italiano, F., & Nuccio, P. M. (1992). Volcanic steam output directly measured in fumaroles: The observed variations at Vulcano Island, Italy, between 1983 and 1987. *Bulletin of Volcanology*, *54*(8), 623–630. https://doi.org/10.1007/bf00430775

Keeling, C. D. (1958). The concentration and isotopic abundance of carbon dioxide in rural and Marin areas. *Geochimica et Cosmochimica Acta*, *13*(4), 322–334. https://doi.org/10.1016/0016-7037(58)90033-4

Keeling, C. D. (1961). The concentration and isotopic abundance of carbon dioxide in rural areas. *Geochimica et Cosmochimica Acta*, *24*(3–4), 277–298. https://doi.org/10.1016/0016-7037(61)90023-0

Lacis, A. A., Schmidt, G. A., Rind, D., & Ruedy, R. A. (2010). Atmospheric CO_2: Principal control governing Earth's temperature. *Science*, *330*(6002), 356–359. https://doi.org/10.1126/science.1190653

Li, G., & Elderfield, H. (2013). Evolution of carbon cycle over the past 100 million years. *Geochimica et Cosmochimica Acta*, *103*, 11–25. https://doi.org/10.1016/j.gca.2012.10.014

Melián, G., Hernández, P. A., Padrón, E., Pérez, N. M., Barrancos, J., Padilla, G., et al. (2014). Spatial and temporal variations of diffuse CO_2 degassing at El Hierro volcanic system: Relation to the 2011–2012 submarine eruption. *Journal of Geophysical Research: Solid Earth*, *119*(9), 6976–6991. https://doi.org/10.1002/2014JB011013

Nuccio, P. M., Paonita, A., & Sortino, F. (1999). Geochemical modeling of mixing between magmatic and hydrothermal gases: The case of Vulcano, Italy. *Earth and Planetary Science Letters*, *167*(3–4), 321–333. https://doi.org/10.1016/S0012–821X(99)00037–0

Oke, T., Mills, G., Christen, A., & Voogt, J. (2017). *Urban climates*. Cambridge University Press. https://doi.org/10.1017/9781139016476

Palano, M., Ferranti, L., Monaco, C., Mattia, M., Aloisi, M., Bruno, V., et al. (2012). GPS velocity and strain fields in Sicily and southern Calabria, Italy: Updated geodetic constraints on tectonic blockinteraction in the central Mediterranean. *Journal of Geophysical Research*, *117*(B7), B07401. https://doi.org/10.1029/2012JB009254

Paonita, A., Favara, R., Nuccio, P. M., & Sortino, F. (2002). Genesis of fumarolic emissions as inferred by isotope mass balances: CO_2 and water at Vulcano Island, Italy. *Geochimica et Cosmochimica Acta*, *66*(5), 759–772. https://doi.org/10.1016/S0016–7037(01)00814–6

Paonita, A., Federico, C., Bonfanti, P., Capasso, G., Inguaggiato, S., Italiano, F., et al. (2013). The episodic and abrupt geochemical changes at La Fossa fumaroles (Vulcano Island, Italy) and related constraints on the dynamics, structure, and compositions of the magmatic system. *Geochimica et Cosmochimica Acta*, *120*, 158–178. https://doi.org/10.1016/j.gca.2013.06.015

Paraschiv, S., & Paraschiv, L. S. (2020). Trends of carbon dioxide (CO_2) emissions from fossil fuels combustion (coal, gas and oil) in the EU member states from 1960 to 2018. *Energy Reports*, *6*(8), 237–242. https://doi.org/10.1016/j.egyr.2020.11.116

Park, R., & Epstein, S. (1960). Carbon isotope fractionation during photosynthesis. *Geochimica et Cosmochimica Acta*, *44*(1–2), 5–15. https://doi.org/10.1016/s0016-7037(60)80006-3

Pataki, D. E., Ehleringer, J. R., Flanagan, L. B., Yakir, D., Bowling, D. R., Still, C. J., et al. (2003). The application and interpretation of keeling plots in terrestrial carbon cycle research. *Global Biogeochemical Cycles*, *17*(1), 1022. https://doi.org/10.1029/2001gb001850

Rogger, J., Hörtnagl, L., Buchmann, N., & Eugster, W. (2022). Carbon dioxide fluxes of a mountain grassland: Drivers, anomalies and annual budgets. *Agricultural and Forest Meteorology*, *314*, 108801. https://doi.org/10.1016/j.agrformet.2021.108801

Sabine, C. L., Feely, R. A., Gruber, N., Key, R. M., Lee, K., Bullister, J. L., et al. (2004). The oceanic sink for anthropogenic CO_2. *Science*, *305*(5682), 367–371. https://doi.org/10.1126/science.1097403

Scoccimarro, E., Gualdi, S., Bellucci, A., Zampieri, M., & Navarra, A. (2013). Heavy precipitation events in a warmer climate: Results from CMIP5 models. *Journal of Climate*, *26*(20), 7902–7911. https://doi.org/10.1175/jcli–d–12–00850.1

Tamburello, G., Kantzas, E., McGonigle, A., Aiuppa, A., & Giudice, G. (2011). UV camera measurements of fumarole field degassing (La Fossa crater, Vulcano Island). *Journal of Volcanology and Geothermal Research*, *199*(1–2), 47–52. https://doi.org/10.1016/j.jvolgeores.2010.10.004

Tarquini, S., Isola, I., Favalli, M., Battistini, A., & Dotta, G. (2023). *TINITALY, a digital elevation model of Italy with a 10 meters cell size (Version 1.1)*. Istituto Nazionale di Geofisica e Vulcanologia (INGV). https://doi.org/10.13127/tinitaly/1.1

Torres, D., Toro, N., Gálvez, E., Castillo, D., Bermúdez, S. A., & Navarra, A. (2022). Temporal variography for the evaluation of atmospheric carbon dioxide monitoring. *IEEE Journal of Selected Topics in Applied Earth Observations and Remote Sensing*, *15*, 80–88. https://doi.org/10.1109/JSTARS.2021.3131414

Umair, M., Kim, D., & Choi, M. (2020). Impact of climate, rising atmospheric carbon dioxide, and other environmental factors on water-use efficiency at multiple land cover types. *Scientific Reports*, *10*(1), 11644. https://doi.org/10.1038/s41598–020–68472–7

Venturi, S., Tassi, F., Cabassi, J., Vaselli, O., Minardi, I., Neri, S., et al. (2019). A multi–instrumental geochemical approach to assess the environmental impact of CO_2–rich gas emissions in a densely populated area: The case of Cava dei Selci (Latium, Italy). *Applied Geochemistry*, *101*, 109–126. https://doi.org/10.1016/j.apgeochem.2019.01.003

Vita, F., Inguaggiato, S., Bobrowski, N., Calderone, L., Galle, B., & Parello, F. (2012). Continuous SO_2 flux measurements for Vulcano Island, Italy. *Annales Geophysicae*. https://doi.org/10.4401/ag–5759

Viveiros, F., Chiodini, G., Cardellini, C., Caliro, S., Zanon, V., Silva, C., et al. (2020). Deep CO_2 emitted at Furnas do Enxofre geothermal area (Terceira Island, Azores archipelago). An approach for determining CO_2 sources and total emissions using carbon isotopic data. *Journal of Volcanology and Geothermal Research*, *401*, 106968. https://doi.org/10.1016/j.jvolgeores.2020.106968

Viveiros, F., Ferreira, T., Cabral Vieira, J., Silva, C., & Gaspar, J. L. (2008). Environmental influences on soil CO_2 degassing at Furnas and Fogo volcanoes (São Miguel Island, Azores archipelago). *Journal of Volcanology and Geothermal Research*, *177*(4), 883–893. https://doi.org/10.1016/j.jvolgeores.2008.07.005

Wimbadi, R. W., Djalante, R., & Mori, A. (2021). Urban experiments with public transport for low carbon mobility transitions in cities: A systematic literature review (1990–2020). *Sustainable Cities and Society*, *72*, 103023. https://doi.org/10.1016/j.scs.2021.103023

Wu, J., Han, Z. Y., Xu, Y., Zhou, B. T., & Gao, X. J. (2020). Changes in extreme climate events in China under 1.5°C–4°C global warming targets: Projections using an ensemble of regional climate model simulations. *Journal of Geophysical Research: Atmosphere*, *125*(2), e2019JD031057. https://doi.org/10.1029/2019JD031057

Xu, L. L., Wang, A. H., Wang, D., & Wang, H. J. (2019). Hot spots of climate extremes in the future. *Journal of Geophysical Research: Atmosphere*, *124*(6), 3035–3049. https://doi.org/10.1029/2018jd029980

Yaacob, N. F. F., Yazid, M. R. M., Maulud, K. N. A., & Basri, N. E. A. (2020). A review of the measurement method, analysis and implementation policy of carbon dioxide emission from transportation. *Sustainability–Basel*, *12*, 14. https://doi.org/10.3390/su12145873

Yakir, D. (2003). The stable isotopic composition of atmospheric CO_2. In H. D. Holland & K. K. Turekian (Eds.), *The atmosphere, treatise on geochemistry* (Vol. 4, pp. 175–212). Elsevier–Pergamon.